January 2015

The Heterotaxy Candidate Gene, Tmem195, Regulates Nuclear Localization Of Beta-Catenin

Anna Ruth Duncan
Yale School of Medicine, annarduncan@gmail.com

The Heterotaxy Candidate Gene, TMEM195, Regulates Nuclear Localization of Beta-catenin

A Thesis Submitted to the
Yale University School of Medicine
in Partial Fulfillment of the Requirements for the
Degree of Doctor of Medicine

By

Anna Ruth Duncan

2015

Abstract

THE HETEROTAXY CANDIDATE GENE, TMEM195, REGULATES NUCLEAR LOCALIZATION OF BETA-CATENIN. Anna R. Duncan, John Griffin, Andrew Robson, and Mustafa K. Khokha. Department of Pediatrics, Yale University, School of Medicine, New Haven, CT.

Congenital heart disease (CHD) affects 1 in every 130 newborns and is the leading cause of infant mortality (2). Heterotaxy (Htx), a disorder of left-right (LR) development, commonly leads to CHD. Despite aggressive surgical management, patients with Htx have poor survival rates and severe morbidity due to their complex CHD. Many of the genetic causes of Htx remain undefined, however, a recent genetic analysis of Htx patients identified a single mutant allele in the novel candidate gene, TMEM195 (3). TMEM195 is an alkylglyercol monooxygenase that cleaves ether lipids, but neither its molecular target nor its role in development has been described (4).

The aim of this project is to identify the molecular mechanism by which TMEM195 alters LR cardiac development. I examined the role of TMEM195 using morpholino (MO) knockdown and mRNA overexpression in *Xenopus tropicalis*. At a low dose of MO, the patient's Htx phenotype was recapitulated in *Xenopus*. At a higher dose of MO, a significant gastrulation defect occurs. Experimental data suggest that the gastrulation defect is secondary to changes in the Wnt signaling pathway. Analysis of TMEM195 knockdown shows a significant decrease in beta-catenin expression and nuclear localization during gastrulation. Nuclear localization

of beta-catenin cannot be rescued by stabilizing beta-catenin, but is rescued by adding a nuclear-localization signal (NLS). These results suggest for the first time that TMEM195 plays a role in the nuclear import of beta-catenin.

TMEM195's role in nuclear localization many not only be specific to Wnt, but may also affect TGF-beta signaling. Smad2 is an important transcription factor for TGF-beta signaling and must be phosphorylated prior to entering the nucleus. TMEM195 depletion leads to an increase in phosphorylated but not total Smad2. In contrast, Smad1 is unaffected. Significantly, both Smad2 and beta-catenin lack NLS signals, while Smad1 has one (5). These results suggest a potentially broader role of TMEM195 in nuclear localization of non-NLS tagged proteins.

Defining the role of TMEM195 will permit a better understanding of the relationship between nuclear localization, gastrulation errors and defects in LR axis development. Importantly, it may also inform our understanding of the currently unknown mechanisms regulating nuclear import of several key signaling factors including beta-catenin and Smad2 and thus pave the way for the development of novel clinical treatments. Both Wnt and TGF-beta signaling are important for a myriad of different disease processes including congenital and vascular malformations, stem cells and cancer.

Acknowledgements

New York Times articles and images line the kitchen cabinets of my childhood home. Teaching me at a young age that women, running, collaboration and never giving up are the answers to the future. One of my favorites reads, “We somehow assume that the gratitude we feel on Thanksgiving applies especially to the largest forms in life. But it applies to the smallest too—to the things we can barely number because we take them for granted.” Thank you to those who have come before me and those who have helped me along the way. I can’t thank my friends, family and mentors enough for their guidance. My progress throughout medical school and my thesis is in great part, due to all of them.

Thank you to my mentor, Mustafa Khokha, who has been motivating, charismatic, and always encouraging. He has taught me not only the basics of developmental biology, but also the best way to approach any scientific question. He is a dedicated physician and scientist, and has been a true role model for my future. I appreciated his trust and support throughout medical school, and have felt fortunate to have him as a mentor. Thank you as well to the Khokha lab post doc, John Griffin, for his collaboration and help. He’s a great friend and scientist, and I have enjoyed learning about the Wnt signaling pathway with him.

Thank you to Andrew Robson and Sarah Moustafa for their preliminary data on TMEM195. Andrew was very thoughtful and encouraging throughout the project, and I can’t thank him enough for his help. Thank you to as well to Florencia del Viso for teaching me about frogs and embryology—I could not have asked for a better mentor my first year in the lab. I’d also like to thank and acknowledge all of the

other Khokha and Brueckner lab members: Maura Lane, Engin Deniz, Emily Mis, Saurabh Kulkarni, Dippy Bhattacharya, Chris Marfo, Davis Li, Sarah Kubek, Mike Slocum, Martina Brueckner, Sveta Makova, Joe Endicott, Shiaulou Yuan, and Jeff Drozd. Thank you for answering all of my questions time and time again and making me feel at home on the fourth floor of FMP.

Thank you to our collaborators in Austria, Ernst Werner and Katrin Watschinger, who provided invaluable discussions and plasmids for our research.

Thank you to the Department of Pediatrics for guidance throughout medical school and the residency match process. In particular, I would like to thank Dr. Brueckner and Dr. Gallagher for their helpful suggestions and for being on my MD/MHS thesis committee. I also thank Drs. Colson, Asnes, Gruen, and Lister for their guidance and support.

Thank you to Dr. Forrest, Mae Geter and Donna Carranzo in the Office of Student Research for their encouragement and endless support. Thank you as well to the NIH for funding my one-year research fellowship through the CTSA TL1 grant.

Thank you to my family and friends for five wonderful and challenging years of medical school. In particular, I would like to thank my parents, Laura Ment and Charles Duncan. From dry ice and soap bubbles in the kitchen sink to coloring at nursing stations on the weekends, they've truly prepared me for a career in both medicine and science.

Thank you to my four older brothers, Pete, Charles, Brian and Andy, who have taught me to always keep up. They have kept me on my toes and inspired me to the next steps. Thank you to my grandmother, who taught me that life exists

outside of the lab and the hospital. I hope to be as caring and witty as she is some day. And of course, thank you to my Poppop, the original Rowe pediatrician.

Finally, thank you to Matthew Marr. Medical school has been a long road, and I have felt fortunate to have you as a classmate, running buddy and friend throughout it all. I look forward to residency with you and all of the next steps in our life.

Table of Contents

1.0 Introduction

1.1 Congenital Heart Disease

Congenital heart disease (CHD) is a major pediatric public health problem. The most common major congenital malformation, CHD affects 9 in every 1000 live births and 1.3 million newborns annually world wide (2). CHD is associated with high rates of morbidity and mortality in those affected and typically requires surgical intervention early in life (6). Finally, the care costs for patients with CHD in the United States exceeds 1.75 billion dollars annually (7).

Recent medical and surgical advances have permitted a greater number of infants with complex CHD to survive to adulthood. There were at least 117,000 adult survivors with CHD living in the U.S. in 2000; this number has increased greatly over the past fifteen years and is predicted to rise by approximately 5% per year (8, 9). Coincident with increasing survival for children with CHD is the recognition of the associated medical and surgical disorders they may harbor. These range from hemodynamic instability and arrhythmias to infertility, pulmonary disease and significant neurodevelopmental disorders (10, 11).

Emerging data suggest that both the rate and type of CHD vary significantly across the world, ranging from 6.1/1000 live births in the U.S. to 9.3/1000 in Asia. Although access to health care may contribute to global differences in CHD, both environmental and genetic factors most certainly play a role (2). In the age of

molecular medicine, identifying those genetic and epigenetic mechanisms responsible for CHD is a priority for both physicians and developmental biologists.

1.2 Congenital Heart Disease and Heterotaxy

Heterotaxy (Htx) is a significant cause of CHD and causes a particularly severe form of CHD. Heterotaxy is an abnormal development of the left-right axis, which leads to incorrect position and organization of the internal organs. The heart, whose function depends on its asymmetry, can be severely affected by abnormal development of the left-right axis (12), and patients with Htx are at high risk for increased post-operative and respiratory complications, arrhythmias, and complications due to other congenital malformations (13, 14). Positioning of the internal organs can be divided into three categories: Situs solitus or a normal positioning of the internal organs; situs inversus, in which the organs are a mirror image; and finally, situs ambiguous, in which there is no clear specificity of the organs along the left-right axis. Htx falls within the category of situs ambiguous. Occurring in 1 in 10,000 newborns, Htx is the cause of 3 % of CHD (12, 15).

Only about 15% of causes of heterotaxy are known to date (16, 17). One commonly studied form of Htx is Primary Ciliary Dyskinesia (PCD). Six to twelve percent of patients with PCD have Htx, (12, 15) and in this disorder the cilia are immotile due to mutations in the inner dynein arms. Cilia are important for establishing the left-right axis of development, and when they are unable to beat, Htx can occur. Work in multiple model systems has elucidated a genetic framework

of embryonic signaling that establishes the LR axis in the developing heart and provides candidate genes, such as DNAH9 in PCD, that are associated with Htx (15, 18).

Unfortunately, much of the genetic burden in heterotaxy remains unexplained at the molecular level despite a sizable array of candidate genes that have been tested (19). Therefore, the Khokha, Brueckner and Lifton labs along with others have initiated human genetic studies on patients with Htx in order to discover the molecular basis of these diseases (3, 16, 20, 21). In 2011, a copy number variant screen by Fakhro *et al* identified variants in 61 genes (3). Further evaluation of these genes showed that 7 were strongly expressed in the left-right organizer of the frog and 5 of 7 initially tested demonstrated severe cardiac looping defects in *Xenopus* (3). Robson, a member the Khokha lab, later examined these 61 genes through an overexpression screen in *Xenopus* and a significant percentage gave cardiac looping defects (unpublished data from Khokha lab). The results of the initial copy number variant and subsequent overexpression screens have identified many new candidate genes and pathways that may be causative of Htx. One of the genes identified by Fakhro *et al* was Transmembrane protein 195 (TMEM195), a gene that currently has no known role in embryonic or cardiac development (3).

1.3 Transmembrane protein 195 (TMEM195/ AGMO)

Fakhro *et al* identified TMEM195 as a candidate gene for Htx in 2011, however, neither its role in development nor its molecular target have been

previously described (3). TMEM195 has been associated with type II diabetes mellitus and insulin resistance in 7 genome wide association studies (GWAS) and intracranial aneurysms in another (22-29). In 2010 TMEM195 was identified as an alkylgycerol monooxygenase (AGMO), an orphan enzyme that is tetrahydrobiopterin dependent and has an iron core (4). AGMO's are necessary for cleaving the O-alkyl bond of ether lipids (Figure 1) (1), and to date TMEM195 is the only AGMO recognized.

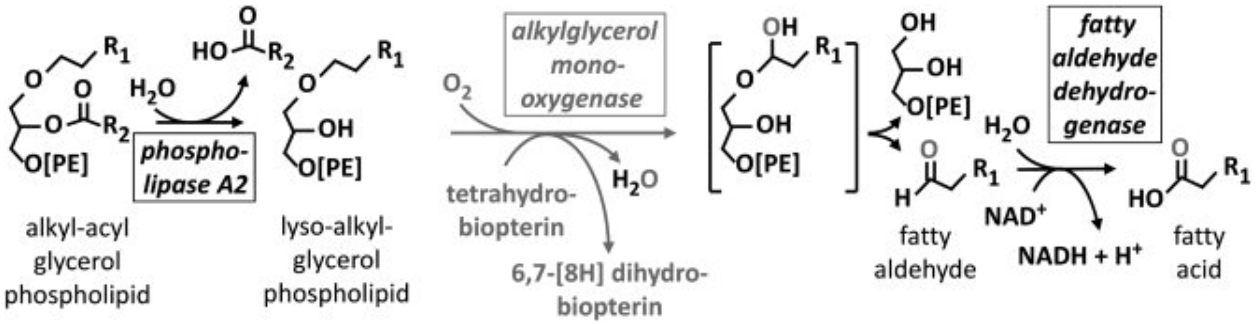

Figure 1: Alkyglycerol monooxygenase reaction (1)

Watschinger and Werner in Austria demonstrated that putative AGMO compounds such as TMEM195 can only cleave specific types of ether bonds. The rules that they and their predecessors established include (1):

(1) No double bond next to the ether-linked fatty alcohol residue at sn1

(2) The fatty alcohol residue at sn1 must have a chain length between 12 and 20 carbon atoms long

(3) The hydroxyl group at sn2 must be free, as with lyso-lipids

(4) Sn2 cannot have acetyl or acyl groups present

(5) Free hydroxyl groups or common phospholipid substitutes are accepted at sn3

(6) The third carbon is not necessary for the reaction to proceed

(7) Phosphate groups cannot be present at the sn3 position (1)

These rules highlight the specific nature of TMEM195; however, to date researchers have not identified a molecular target for this catalytic site. They believe that it maybe acting at the level of the endoplasmic reticulum, since they have shown its localization there in transfected CHO cells (4).

TMEM195 is well conserved across species ranging from *C. Elegans* to zebrafish, *Xenopus*, rodents and humans. Due to TMEM195's extreme instability, the protein structure has not been ascertained experimentally. Instead, the Werner lab predicted the structure of TMEM195 using the Rosetta membrane protein prediction tools (Figure 2, adapted from (1)). TMEM195 is believed to be 445 amino acids long and contains 5 membrane-spanning sections and a non-membrane associated helix. Amino acids 132 through 244 are required for enzymatic cleavage. Wastchinger et al identified this region through a mutagenesis screen. The region contains one glutamate with which the co-factor tetrahydrobiopterin can bind, eight histidine residues within the fatty acid motif, and three additional amino acids, all of which are necessary for catalytic function (4).

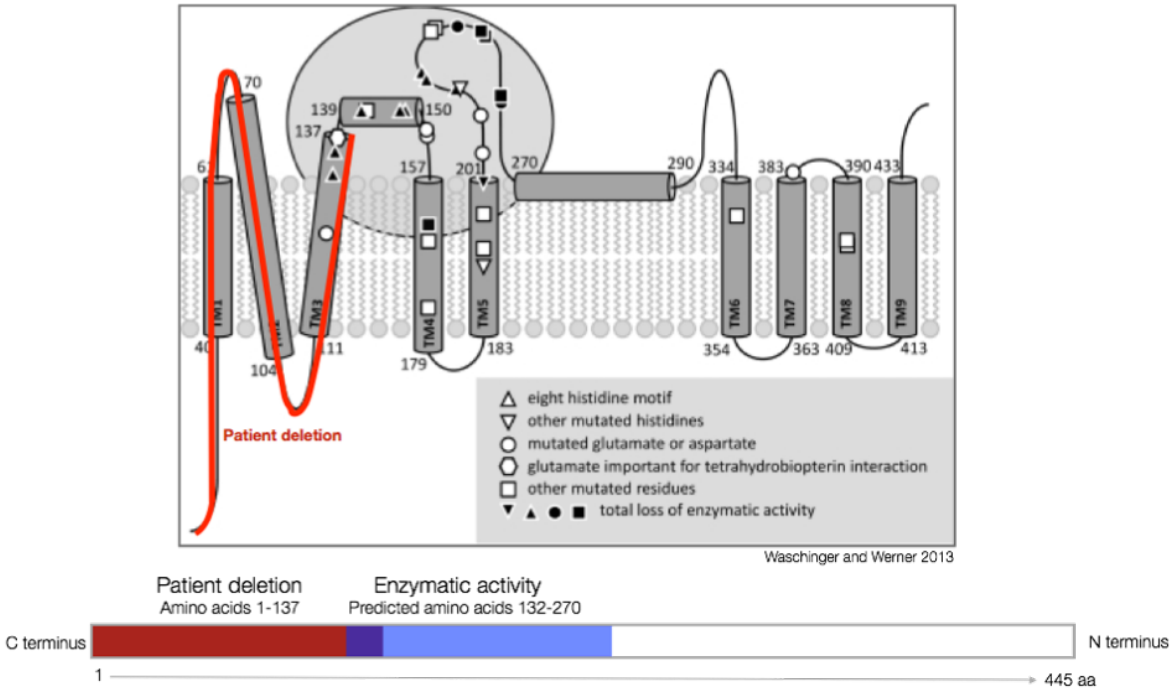

Figure 2: Schematic of TMEM195's predicted protein structure.

In Fakhro *et al's* study, the Htx patient's variant was a deletion between amino acids 1 through 137; thus this deletion putatively disrupts the region necessary for enzymatic activity (1, 3, 4).

While there may be a biochemical role for TMEM195, the physiologic role of TMEM195 remains undefined. To address this further, one can examine the role of ether lipids in physiology to determine if developmental processes may overlap. Ether lipids are found primarily within lipid membranes. There are several types of ether lipids based on chemical structure. The first is 1-*O*-alkyl-*sn*-glycerol lipids or plasmanyl-phospholipids, which are a group of lipid mediators that include platelet-activating factor. The second type is 1-*O*-(alk-1′-enyl)-*sn*-glycerols, which make up much of the lipid membranes in animals. The third is 1-*O*-(alk-1′-enyl)-*sn*-glycerols

or plamalogens, which are important for membrane fluidity, membrane fusion, myelination, and spermatogenesis. Finally, (2′*R*)-1-*O*-(2′-methoxyalkyl)-*sn*-glycerols or methoxylated alkyglycerols comprise the fourth type; they have been isolated from many organisms, including the livers of sharks, and are thought to inhibit tumor growth (30). Types 1, 2, and 4 are all possible substrates for TMEM195; however, type 3 cannot be since it has a double bond present next to the ether linkage (4).

This classification of ether lipids helps one to hypothesize what TMEM195's target may be. These include a lipid signaling mediator, a molecule involved in carcinogenesis, a component of a lipid raft or a GPI anchor, but it is unlikely to be involved in membrane fusion or myelination. The possibilities are numerous, but the rules outlined by Watschinger, Werner and colleagues help to frame a network by which to analyze them.

Other than its biochemical activity, very little is known about TMEM195 to date. Fakhro *et al's* findings suggest that TMEM195 plays an important role during development, helping to establish left-right patterning and heart development. However, the molecular mechanism by which this occurs has not yet been established and is key to understanding the index patient's phenotype.

1.4 *Xenopus* as a model organism for human disease

The frog model, *Xenopus tropicalis,* is a rapid, efficient, and *in vivo* system to study left-right patterning and cardiac development (31, 32). There are two types of

Xenopus typically used in developmental biology—*X.* l*aevis* and *X. tropicalis*. *X. laevis* is an allotetraploid and *X. tropicalis* is a diploid, making *X. tropicalis* a more appropriate organism for genetic modification. *Xenopus* embryos can be easily generated in large numbers. Hundreds of synchronized embryos can be injected at cleavage stages after *in vitro* fertilization. Then, just three days later, cardiac looping can be examined by simply looking at the heart through transparent skin. Microinjection of embryos is straightforward, and mRNA or morpholinos (MOs) can be used for gain or loss of function studies, respectively. By targeting one cell at the two-cell stage, the right or left side of the embryo can be manipulated, while the other side serves as an internal control. This is not possible in other heterotaxy disease models. Lastly, *Xenopus* is the closest vertebrate model to humans that retains the advantages of speed and cost when compared to zebrafish and mouse. For all of these reasons, *Xenopus* is an ideal system to model human congenital heart disease.

1.5 The Left-Right Organizer in LR patterning

Studies in many developmental model organisms have identified a conserved LR patterning program that determines proper cardiac situs. During gastrulation, asymmetric development begins at the left-right organizer (LRO; mouse node, zebrafish Kuppfer's vesicle, and gastrocoel roof plate [GRP] in frog; shown

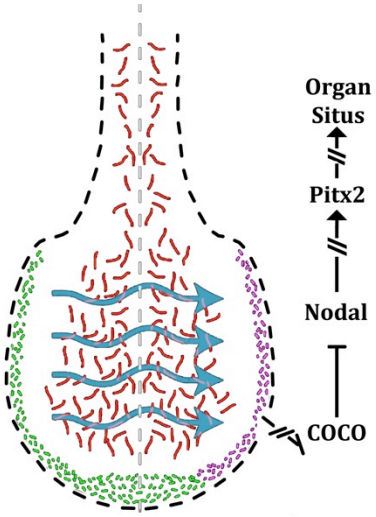

Figure 4: Left-right organizer

in figure to the right), which forms in the dorsal posterior region of the embryo. In cells of the LRO, motile monocilia beat to create a leftward flow in the extracellular fluid of the LRO (33, 34). According to the two cilia model, immotile cilia on surrounding cells act as sensors, detecting the flow and eventually translating it into asymmetric gene expression. Coco (CERL2), a nodal antagonist, is one of the earliest genes that is asymmetrically expressed and eventually transmits the LRO asymmetry to the left lateral plate mesoderm via phosphorylated-Smad2 activating Pitx2 (35, 36). Pitx2 is also involved in the organogenesis of the heart, gut and lungs (37, 38). Following activation of these developmental pathways, cardiac precursor cells that first form in the midline as a straight heart tube are then looped to the right, establishing cardiac asymmetry. In addition to the nodal cascade a number of other signaling pathways have been implicated in LR patterning (39).

1.6 Initiation of dorsal ventral patterning

As discussed in detail below, TMEM195 depletion affects gastrulation and dorsal ventral patterning. To provide context, I will briefly review dorsal ventral (DV) patterning in developing embryos. DV patterning is established as soon as the sperm enters the oocyte. The sperm entry point marks the ventral side of the embryo, and the opposite side will become the embryo's dorsal side. Once the sperm enters, cortical rotation takes place, during which a microtubule array helps the cortical cytoplasm to rotate 30 degrees with respect to the internal cytoplasm. This rotation creates the grey crescent. The grey crescent is key in establishing dorsal

ventral patterning because not only does the first cleavage bisect the grey crescent, but also gastrulation will take place in this location. Therefore, establishing the dorsal side of the embryos begins at fertilization. Further signals will propagate this message as the embryo grows and divides (40).

1.7 Dorsal ventral patterning during gastrulation

Gastrulation is the process by which the embryo involutes to form its distinct cellular germ layers—endoderm, mesoderm and ectoderm. Each of these cellular layers influences one another and sends signals that differentiate the embryonic tissue further by activating different genetic expression patterns. This important involution of dorsal tissue begins at stage 10 in *Xenopus* at the site of the grey crescent, now called the blastopore lip. The blastopore lip is within the marginal zone of the embryo—the region where the animal and vegetal poles meet (40).

Spemann and Mangold were the first to show that the blastopore lip is essential for determining cell fate (40). They performed dorsal marginal zone transplantation experiments and demonstrated that gastrulation could be initiated in a new region of the embryo. This transplanted tissue acted like an organizer, because it was able to induce the host tissue to change its cellular fate. Subsequently Nieuwkoop showed that the vegetal cells below the ectoderm were able to induce the ectoderm to become mesodermal cells including dorsal mesoderm. Further experiments demonstrated that beta-catenin, a key member of the Wnt signaling family, enabled this vegetal cell activity (40).

1.7.1 Wnt signaling

Wnts are cysteine rich, evolutionarily well-conserved proteins that activate signaling cascades (41). Nineteen different Wnts have been identified to date (41). There are two major pathways activated by Wnts, the canonical and the non-canonical Wnt signaling cascades. The canonical pathway is the beta-catenin dependent pathway, central to this thesis; the non-canonical is the beta-catenin independent pathway.

The canonical pathway has both active and inactive states (Figure 7c). In the absence of Wnt activation, beta-catenin is bound to the degradation complex formed by APC, axin and GSK3. GSK3 enables the formation of this degradation complex by phosphorylating both axin and beta-catenin and allowing them to interact. The phosphorylation of beta-catenin also targets beta-catenin for degradation by ubiquitin and the proteasome (42). This ultimately prevents beta-catenin from accumulating in the cytoplasm and translocating into the nucleus.

In the active state, Wnt binds to the cellular receptor Frizzled (Fz) though Fz's cysteine rich extracellular domain, leading to di-sulfide bonds between the two molecules (41). LRP6, a single pass transmembrane protein, is then recruited to form a ternary structure with both Fz and Wnt (41). DSVL binds to this complex and, since it is oligomerized, facilitates clustering of the complexes to form signalosomes (41). The intracellular domain of LRP6 is then phosphorylated by CK1-y. This phosphorylation is important because it recruits phosphorylated-Axin along with the other members of the degradation complex, APC, GSK3 and beta-catenin (41, 42). Phosphorylated LRP6 inhibits GSK3, preventing it from

phosphorylating beta-catenin and targeting it for degradation (42). Once GSK3 is inhibited, Axin can be dephosphorylated by the phosphatase, PP1. This dephosphorylation of Axin encourages Axin to undergo a conformational change, becoming inactive, and unable to bind with beta-catenin or LRP6 (42). Beta-catenin is then released and able to accumulate in the cytoplasm and later translocate into the nucleus (discussed in further detail below).

In the early embryo beta-catenin is critical for dorsal ventral patterning. During gastrulation beta-catenin is predominately localized within the nuclei of the dorsal blastopore lip. In the nucleus, beta-catenin binds to T cell factor and lymphoid enhancer binding-factor, leading to activation of genes such as Twin, Siamois, Xnr3 and other Spemann Organizer genes, which are necessary for dorsal structure formation. Depletion of beta-catenin leads to ventralization of the organism; no dorsal structures, such as a head or neural tube, will form when beta-catenin is depleted (43). In contrast, overexpression of beta-catenin leads to secondary axis formation; these embryos form conjoined twins with two neural tubes and two heads (44).

During development, beta-catenin is initially a product of maternal mRNA. The cytoplasmic movements that create the grey crescent also cause Wnt signaling to be activated on the embryo's dorsal side. The microtubule array of the embryo is responsible for directing Wnt11, GSK3-binding protein (GSK3-BP) and disheveled (DSVL) from the vegetal to the dorsal side of the embryo. GSK3-BP and DSVL then stabilize beta-catenin in the cytoplasm of dorsal cells and prevent it from being degraded (40). Subsequently, beta-catenin is able to translocate into the nucleus

and up-regulate dorsal gene expression. Wnt11 is also up-regulated in the dorsal region of the embryo, and its role is to activate Wnt signaling on the dorsal side of the embryos, leading to an increase in nuclear beta-catenin localization (40).

1.7.2 TGF-beta Signaling and Smad2

Transforming growth factor-beta (TGF-beta) is a family of growth factors with greater than 40 members with diverse roles ranging from embryonic development to cell proliferation, apoptosis and angiogenesis (45). One of the earliest roles of TGF-beta signaling is mesoderm formation and activation of genes in the left-right organizer (40).

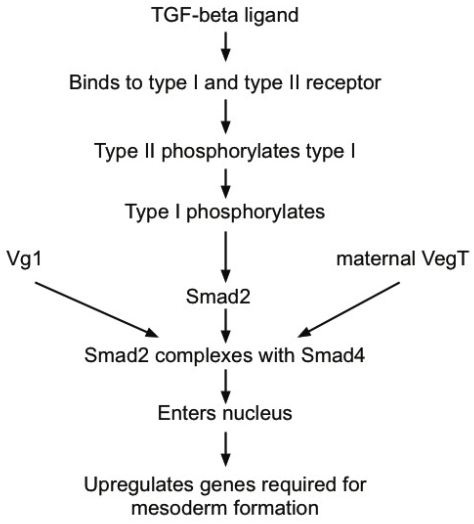

Figure 3: TGF-beta signaling pathway

TGF-beta ligands, such as nodal, act by binding to and bringing together the types I and II serine/ threonine kinase receptors on the cell surface (45). The type II receptor phosphorylates the type I receptor, which in turn phosphorylates Smad family members. Smads 1 through 6 and 8 act as transcription factors of the TGF-beta family. Notably, Smad2 plays a role in mesoderm induction during embryonic development (40). Phosphorylated Smad2 complexes with Smad4 to enter the nucleus and act as a transcription factor (45).

In order for Smad2 to become activated, it must be phosphorylated. As shown in the flow chart, it is activated by either Nodal-related paracrine factors, Vg1

or the maternal VegT, which are secreted by vegetal cells below the endoderm. Secretion of the nodal-related paracrine factors is partially due to beta-catenin, which may lead to a gradient of phosphorylated-Smad2, with higher amounts of phosphorylated-Smad2 likely expressed dorsally (40). Early on, activated phosphorylated-Smad2 is essential for mesoderm induction. While later, it is necessary for LR asymmetry in the lateral plate mesoderm (39, 46).

1.8 Nuclear localization

As discussed above, it is essential for both beta-catenin and Smad2 to enter the nucleus in order for them to bind transcription factors and regulate target genes. This section will focus on both the canonical nuclear localization pathway and hypothesized alternatives to that route.

1.8.1 Canonical nuclear localization

One way in which proteins can be transported from the cytoplasm to the nucleus is through a nuclear localization signal (NLS). An NLS signal is a group of amino acids that is recognized by importin-alpha. Importin-alpha can then bind to importin-beta, which can transport itself and its cargo into the nucleus. Some Importin-betas can also bind directly to NLS signals without the importin-alpha intermediate (5). After binding to the cargo in the cytoplasm, importin-beta interacts with the FG repeats of nuclear pore proteins. The FG repeats of the nuclear pore protein interact with the HEAT repeats, a set 39 amino acids repeated 19 times

on importin-beta (47). Once importin-beta is within the nucleus Ran-GTP binds to it, which causes a conformational change and the release of the cargo from importin-beta (47).

1.8.2 Nuclear import of beta-catenin:

Canonical nuclear localization is an elegant pathway, by which proteins can enter the nucleus, but not all proteins contain NLS signals and how they enter and exit the nucleus is undefined. An active mechanism is necessary as many proteins are too large to simply diffuse into the nucleus. Beta-catenin and Smad2 are two such proteins (5). Much research has focused on the nuclear localization of beta-catenin and Smad2; currently the only consensus is that the importin-beta-Ran pathway is not involved.

Once beta-catenin is released from the Wnt degradation complex, it is able to accumulate in the cytoplasm and eventually translocate into the nucleus. Many hypotheses exist for the nuclear translocation mechanism, including calcium gradients, interactions with nuclear pores and binding partners.

The first hypothesis is that a calcium surge causes beta-catenin to be imported into the nucleus. Thrasivoulou et al showed that Wnt ligands stimulate a calcium release, causing an increase in intra-nuclear calcium and a depolarization of the nuclear membrane. As nuclear calcium levels rise, nuclear localized beta-catenin increases as well, suggesting that depolarization of the membrane is necessary for beta-catenin, a large and negatively charged molecule, to be imported (48). This model explains the electrical currents at play, but does not explain how

beta-catenin enters through the nuclear membrane, since it is too large to diffuse and does not bind to importin-alpha or beta.

The second hypothesis is that beta-catenin interacts independently with nuclear pore proteins. Fagotto *et al* have shown that beta-catenin can dock at the nuclear pore and that the docking location competes with importin-beta. Their experiment showed interactions between beta-catenin and the yeast Nup1 (49). Later experiments have shown interactions between the hydrophobic N- and C-terminal tails and the Armadillo repeats of beta-catenin with Nups 62, 98, 153 and 358 (50). Nup358 contains cytoplasmic filaments, Nup62 represents part of the central channel, and Nups 98 and 153 represent parts of the nuclear pore basket. In this model, beta-catenin may sequentially bind nuclear pore components in order to be imported (50). A fundamental weakness of all of these studies is that to date no known report identifies a protein that directly regulates nuclear transport of beta-catenin. My study is the first to identify just such a protein, TMEM195.

1.8.3 Nuclear import of Smad2

Once Smad2 is phosphorylated, it is able to go into the nucleus. Many of the Smad transcription factors have NLS signals, but Smad2 does not. Smad2 forms a complex with Smad3 and Smad4, so one initial hypothesis was that Smad3 or 4 can carry Smad2 into the nucleus through the canonical NLS pathway (51). However, this is no longer the prominent belief in the Smad field, since research has shown that Smad2 can interact directly with nuclear pore proteins, independent of importin-beta (47). Massague, Xu and colleagues have shown that Smad2's

hydrophobic MH2 domain can bind to CAN/Nup214 and Nup153 (47, 52). The MH2 domain also has binding partners in the cytoplasm, SARA, and nucleus, Fast-1. The nuclear pore proteins are therefore thought to compete with SARA and Fast-1 for Smad2 bind, creating a balanced flux between the cytoplasm and nucleus. In this model, when the TGF-beta pathway is activated more Smad2 will be phosphorylated. SARA, the cytoplasmic binding partner, has a lower affinity for phosphorylated Smad2, allowing Smad2 to bind to Nup214 or 153 and enter the nucleus (53-55). This model does not explain how Smad2 is released from the nuclear pore; it simply implies that its release is based off a higher affinity for its nuclear binding partners. This research also suggests that the more Smad2 is phosphorylated, the greater its affinity for Smad4, one of its transcriptional complex partners (47). After nuclear entry, an additional phosphorylation or modification event may be necessary for Smad2's release into the nucleus.

Another possible mechanism for nuclear localization of Smad2 is through the transcription factor TAZ (56). TAZ can bind to phosphorylated-Smad2 through its MH1 domain in either the cytoplasm or nucleus. When TAZ levels were modulated between the nucleus and cytoplasm, Smad2 localization was affected, suggesting that TAZ and Smad2 localization are linked. Though this model does suggest a novel shuttling partner for Smad2, it does not elucidate the mechanism by which it shuttles into and out of the nucleus.

1.9.4 Nuclear import of proteins containing Armadillo repeats

One model proposed by Fagotto and Massague suggests that beta-catenin, Smad2 and Erk2, another transcription factor not discussed here, may all have similar mechanisms of nuclear import (5, 49). Their theory is that beta-catenin, Smad2 and Erk2 can all act like importin-beta, because they have Armadillo repeats, which are very similar to the HEAT repeats described in importin-beta. This means that an NLS signal would not be needed for any of these transcription factors to enter the nucleus; their armadillo repeats would simply bind to the FG repeats of the nuclear pore (5). A not yet identified small GTPase may then be needed to release the transcription factor into the nucleus or another not yet identified protein may be necessary for its cleavage or release (49).

This hypothesis seems both reasonable and testable, given that beta-catenin and Smad2 can bind to nuclear pore proteins. It therefore suggests the framework for a parallel pathway, in which beta-catenin and Smad2 can act as their own importin-betas for shuttling. Questions, however, still remain—such as how are beta-catenin and smad2 released into the nucleus and whether or not they have binding partners during their nuclear shuttle. Though many questions persist, my research on TMEM195 helps to bridge this knowledge gap. This project has led to the identification of a new component of the Wnt signaling pathway that appears to affect beta-catenin nuclear transport, identifying one of the first factors to do so.

2.0 Statement of Purpose

2.1 Specific aims:

1. *Determine the role of TMEM195 in left right patterning.*

   TMEM195 was identified in an index patient with heterotaxy and CHD. Currently there is no known functional role of TMEM195 in left-right patterning or during development. TMEM195 will be analyzed in the rapid vertebrate model *Xenopus*.

   1A: Examine whether TMEM195 alters heart situs.

   1B: Test sequential steps in the left-right signaling cascade to interrogate the functional role of TMEM195.

   Successful completion of this Aim will determine at what points in the left-right pathway TMEM195 is acting.

2. *Define the role of TMEM195 in gastrulation*

   TMEM195 depletion significantly impairs gastrulation. Successful completion of this Aim will define the mechanism by which TMEM195's role in gastrulation leads to defects in left-right patterning and cardiac development.

The goals of this proposal are to establish a functional role for TMEM195 in LR development and to elucidate the molecular mechanisms by which this orphan

enzyme acts. By doing so, additional evidence will be garnered to support TMEM195 as a Htx disease causing gene and further improve understanding of CHD. Aided by information about the molecular mechanisms contributing to CHD, future physicians and scientists will be able to personalize the treatment plans of these children. CHD can be devastating for the child and the family, but because of emerging surgical improvements, many affected children now survive. Clinically, however, two children with very similar phenotypes can have very different outcomes. With a genetic test in hand, pediatricians and cardiologists of the future will know whether these outcomes were due to molecular differences and will be able to predict and optimize care. The overarching goal of this project is to elucidate the molecular mechanisms contributing to CHD, so that future treatment can be individualized for each affected child.

2.2 Hypotheses:

1. Depletion of TMEM195 leads to abnormal cardiac looping.
2. TMEM195 affects LR patterning by altering Wnt signaling in particular the nuclear transport of beta-catenin.

3.0 Methods

3.1 Embryo manipulation

3.1.1 *Xenopus* husbandry

Xenopus tropicalis were housed and cared for by lab members in the aquatics facility at Yale. Animals were taken care of according to established IACUC protocols.

3.1.2 In-vitro fertilization of *Xenopus tropicalis*

Females were primed the evening before injections with 10 units of HCG. Females were then boosted 4 hours prior to injections with 200 units of HCG. Just prior to injecting, the male was euthanized with benzocaine and his testes removed. Eggs were obtained from the female, and then the sperm solution (from crushed testes) and eggs were mixed in a petri dish. The sperm and eggs were incubated together for 3 minutes, allowing the sperm time to attach to the eggs. The petri dish was then flooded with 0.1 X MBS and allowed to sit for 10 minutes. Once all of the animal pole of the eggs had constricted, denoting fertilization, the eggs were rinsed in cysteine, which breaks apart the thick jelly coats of the eggs. After 5 minutes, the cysteine was rinsed off by a series of washes with 0.1X MBS and then the eggs were left in 3% ficoll in 1/9 X MR for injecting (57).

3.1.3 Microinjections of morpholino or mRNA in Xenopus

Embryos were injected with either a morpholino (MO) for TMEM195 or an mRNA at the one or two cell stage. Embryos were injected according to an established protocol in which a picospritzer and micromanipulator holding fine injection needles was used to inject 2 microliter of solution per embryo (58). The MO injected was from Gene Tools and has the following sequence, 5' GGCCTGTGAAACCCCCCATGTTTGC 3'. 1ng of MO was injected for the low dose Htx experiments, and 2ng was injected for the high dose gastrulation experiments. The MO was traced with mini ruby dye (Invitrogen). 300pg of TMEM195-GFP mRNA was injected for rescue of the gastrulation mutants, and for the secondary axis assay. 300pg was also injected of TMEM195-H136A-GFP, TMEM195-H149A-GFP as a comparison (generously provided by Ernst Werner in Austria).

Secondary axis assays and nuclear localization studies utilized 200pg of GFP-beta-catenin (Addgene #16839), Stabilized-beta-catenin (Addgene #29684), and NLS-beta-catenin (Addgene #29684), and each was co-injected with 200pg of NLS-mCherry (Addgene #49313).

Embryos were then collected according to Nieuwkoop and Faber staging (59). I performed all injections either independently or in collaboration with John Griffin, Andrew Robson and Mustafa Khokha.

3.1.4 Cardiac looping

Frog embryos were scored at stage 45 of development. Embryos were treated with benzocaine and scored ventrally with a light microscope. Looping was

determined based off of position of the outflow tract. A D-loop was defined as the outflow tract going to the right, an L-loop was to the left, and an A-loop was midline. I independently scored all cardiac loops. Ambiguous loops were re-scored by additional lab members for verification.

3.15 Gastrocoel roof plate explants

Gastrocoel roof plates (GRPs) were dissected for use in the whole mount *in-situ* hybridization protocol. GRPs were dissected at stages 14, 16 and 19, by bisecting the embryo and then removing the posterior dorsal tissue that makes up the GRP. Dissection knives, forceps and homemade hair-tools were utilized.

3.1.6 Blastopore lip explants

Blastopore lips were removed from GFP-injected embryos at stages 10 through 12 with a dissecting knife and forceps under a light microscope. These explants were fixed with 1x MEMFA and stained with the nuclear stain DAPI. Then visualized under the confocal microscope. These explants were used for nuclear localization of beta-catenin.

3.1.7 Secondary axis assay

For the secondary axis assay, embryos were injected at the one cell stage with wild type-beta-catenin, stabilized- beta-catenin, or NLS- beta-catenin. A subset of each group was then injected with the either TMEM195 MO or GSK3 mRNA. Embryos were collected at stage 19 and scored for either a primary or secondary

axis, based off of the presence of one or two neural tubes. Both John Griffin and I scored each of the secondary axes for verification.

3.2 Molecular and cellular techniques

3.2.1 Whole mount *in-situ* hybridization

In-situ hybridization was performed as previously described (58). Digoxingenin labeled anti-sense RNA probes were made using a T7 mMessage mMachine transcription kit (Ambion #AM1344). Probes for Coco, Xnr1, Gdf6 and Pitx2 were made using clones TEgg007d24, TGas124h10, Tgas137g21, and TNeu083k20. Probes were hybridized, stained with appropriate anti-digoxingenin secondary antibody, then fixed in bouin's fixative, washed in SCC buffer, bleached and dehydrated in 100% ethanol according to the detailed previously described protocols (58, 60).

3.2.2 Immunohistochemistry

Embryos were collected at stage 16, then fixed for 1 hour in 1x MEMFA. GRP explants were dissected as previously described, then blocked in 5% BSA for 1 hour. Primary antibody for detecting cilia (Acetylated tubulin Sigma #T6793) was subsequently left on overnight at 4 degrees at a concentration of 1:2000. Embryos were then washed several times with 1x PBS before being incubated in secondary antibody (Alexa 488 goat anti-mouse IgG, Invitrogen #A1101 1:2000) for 1 hour at room temperature. Embryos were then washed and mounted, as described below.

3.2.3 Protein extraction

Embryos were collected at stages 9-12, and homogenized in 1x RIPA buffer (100 microliter per 10 embryos) to extract protein. Protein extracts were centrifuged at 4 degrees for 20 minutes. The middle layer was removed (this excluded the pellet and fat layers), and centrifuged for 10 more minutes at 4 degrees. The middle layer was once again removed and frozen at -80 degrees.

3.2.4 Western blots

Western blots were performed using 4-12% Tris-Bis gels, gel chamber and semi-dry transfer module from Invitrogen according to Invitrogen's established protocol. Once transferred, PVDF membranes were blocked with 5% milk or BSA for 1 hour followed by primary antibody at 4 degrees overnight. Primary antibodies used include anti-Beta-catenin H-102 (Santa Cruz sc-7199) at 1:1000, anti-Gapdh (Ambion #4300) at 1:2000, anti-Smad1 (Cell Signaling #9743) at 1:2000, anti-phospho-Smad1 Ser 463/465 (Cell Signaling #9511) at 1:2000, anti-Smad2 (Cell Signaling #3122) at 1:2000, and anti-phospho-Smad2 (Cell Signaling) at a 1:2000 concentration.

Membranes were then washed in 1x TBST and incubated in secondary for 1 hour at room temperature. Secondary antibodies used were HRP conjugated and include Peroxidase-conjugated Affinipure Donkey Anti-mouse 1gG (Jackson ImmunoResearch laboratory #715-035-150) at 1:10,000 and Peroxidase conjugated IgG Fraction Mouse Anti-rabbit IgG (Jackson ImmunoResearch laboratory #211-032-171) at a 1:15,000 concentration.

Membranes were then washed in TBST and developed with Amersham ECL Western Blot Detection Reagents (GE Healthcare).

Western blots were quantitated using NIH's software ImageJ as a ratio of experimental antibody to the control (Gapdh), and then as a ratio of the injected to the uninjected control.

3.2.5 TOPflash assay

TOPflash was used to measure downstream activity of the Wnt signaling pathway. Embryos were injected with the Top and Renilla plasmids. The Top plasmid has TCF binding sites upstream of a minimal reporter and the firefly luciferase gene. When TCF activates transcription of Wnt targets it will also cause Top to make luciferase. The internal control is the Renilla plasmid, in which Renilla luciferase production is driven by a control promoter whose activity should be the same in all cells. A separate sample is injected with Fop and Renilla. In Fop, the TCF binding sites are mutated so it's a negative control. Finally, enzymes are added, which causes the luciferase to produce light, which can be measured on a luminometer and be quantified (Promega Dual Luciferase Reporter Assay System #E1910).

Half of the embryos injected with the Top and Renilla plasmids were also co-injected with either the TMEM195 MO or mRNA. Each experiment used three biological samples and repeated the measurements in triplicate. Patrick Gallagher and his lab at Yale generously provided the luciferase software and guidance. TOPflash assays were performed in collaboration with John Griffin.

3.2.6 Nuclear localization

Nuclear localization studies were performed to look at the presence or absence of beta-catenin in the nucleus. Embryos were injected with GFP tagged wild type beta-catenin or NLS-beta-catenin and NLS-mCherry. Half of the samples were then injected with 2ng of the TMEM195 MO and mini ruby tracer. Embryos were raised until stages 9-12, then collected, fixed in 1x MEMFA for 1 hour and dissected as described above. Embryos were washed in 1x PBS and stained for 10 minutes with the nuclear stain DAPI. Embryos were then mounted and examined under the confocal microscope.

3.3 Imaging

3.3.1 Mounting slides

Embryos were mounted on coverslips following dissection and staining protocols. Explants were placed on a coverslip and all liquid was removed. 80-100 microliters of mounting media (Prolong-gold) was then applied, and then a coverslip was carefully placed over the explants.

3.3.2 Confocal imaging

The Zeiss LSM 710 microscope in Yale's core facility was used for all confocal imaging. Consistent laser power and microscope settings were used for each image and experiment. Images were taken with the assistance of John Griffin.

3.4 Statistical analysis

This was a prospective study that utilized *Xenopus* as a model system for development. Embryos were randomly selected from a fertilized population and utilized for injections, scoring or collection. A sample number was reported for each experiment. Each experiment was performed at least 3 times unless otherwise stated. The statistical significance of each experiment was examined using a chi-square analysis with Yates correction. In all figures and results, statistical significance was defined as $p < 0.05$.

With the guidance of Khokha lab members, I independently performed each of the protocols listed above, unless stated otherwise.

4.0 Results

4.1 Heterotaxy phenotype: low dose TMEM195 depletion leads to heterotaxy

Since the identified patient had a deletion of TMEM195, I used a morpholino (MO) to knockdown TMEM195 protein expression. Cardiac looping in the embryos was examined in order to determine if this patient's phenotype was recapitulated in *Xenopus* (Figure 5a). Three days after fertilization and at stage 45, the hearts of *X. tropicalis* embryos are easily visible through the embryos skin and can be scored for cardiac looping. Typically the outflow tract loops to the right, creating a D-looped

heart, however, if a low dose (1ng) of TMEM195 MO is injected at the one cell state, only 78% have D-looped hearts, while 20% of embryos display L-loops or a leftward looping outflow tract, and 2% have A-loops or mid-line outflow tract (n =130). This is in comparison to uninjected control embryos, in which 99% have D-loops, 1% L-loops and 0% A-loops (n= 230). At the two-cell stage, 1ng of TMEM195 MO can be injected into one of the two cells, and embryos can be selected that affect only the right or left side. If the MO targets the right side, 67% have D-loops, 33% L-loops and 0% A-loops (n= 18). If the MO is injected into the left side, 46% have D-loops, 46% L-loops and 9% A-loops (n = 33). The difference between uninjected controls and TMEM195 depleted embryos injected at both the one and two cell stages was statistically significant, with a p value < 0.001.

Since TMEM195 knockdown embryos have abnormal cardiac looping, I examined Pitx2, an upstream marker of organ situs (Figure 5b). Pitx2 is typically expressed in the left lateral plate mesoderm of embryos prior to organ situs determination. In the uninjected control embryos, 95% of embryos had Pitx2 expressed on the left side and 5% had abnormal pitx2 expression, with 3% expressed on the right and 2% absent bilaterally (n = 63). When TMEM195 was knocked down with 1ng of MO, 75% of embryos had normal left sided Pitx2 expression, 25% of embryos had abnormal Pitx2 expression, with 5% on the right, 7% bilateral and 13% absent (n = 80). Results show a statistical difference between normal versus abnormal Pitx2 expression in the wild type versus knockdown embryos with a $P < 0.02$.

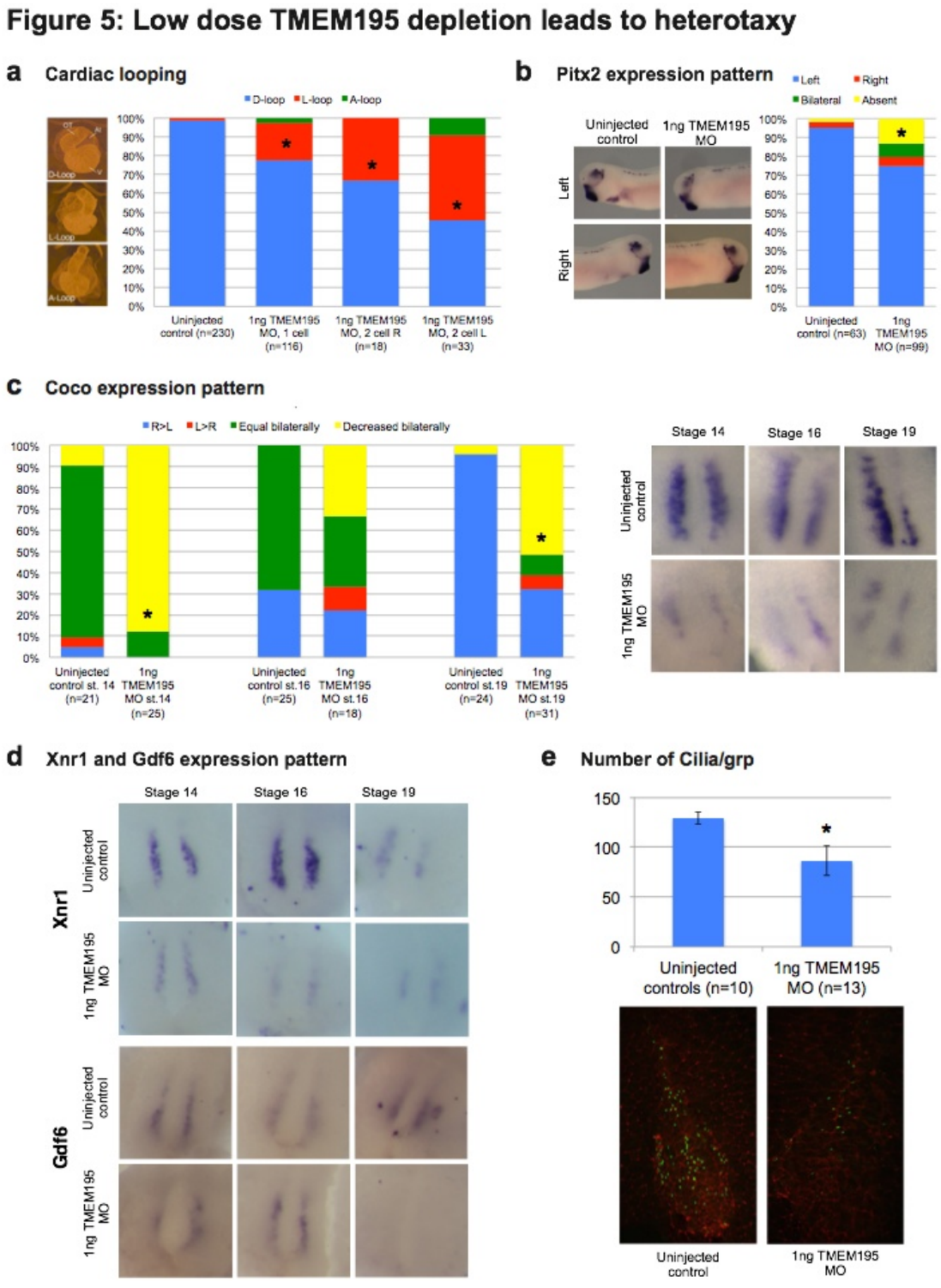

Figure 5: Low dose TMEM195 depletion leads to heterotaxy.
a) Cardiac looping at stage 45 of development with * equal to $P < 0.001$. b) Expression pattern of Pixt2 at stage 28 of development with * equal to a $P < 0.02$. c) Expression pattern of Coco in GRPs at stages 14, 16 and 19 of development with * equal to $P < 0.001$. d) Expression pattern of Xnr1 and Gdf6 in GRPs at stage 14, 16 and 19 of development. e) Number of cilia per GRP counted at stage 16 of development with * equal to $P < 0.001$.

Since Pitx2 expression is abnormal in TMEM195 knockdown embryos, I examined Coco, an early marker in the left-right cascade. Coco is typically expressed bilaterally in the Gastroceol roof plate or left-right organizer (GRP) of embryos at stage 14 (Figure 5c). At stage 16, when nodal flow begins, Coco is repressed on the left side of the GRP, making Coco expression greater on the left than the right of the GRP. This difference between left and right sides of the GRP is more obvious at stage 19. In uninjected control embryos, 81% have normal bilateral Coco expression at stage 14, 5% have right greater than left, 5% have left greater than right and 10% were decreased bilaterally (n = 21). In TMEM195 knockdowns at stage 14, 12% have equal bilateral expression, 0% have right greater than left, 0% have left greater than right and 88% are decreased bilaterally (n = 25). At stage 14, normal versus abnormal Coco expression is statistically significant with $P < 0.001$. In uninjected control embryos at stage 16, 32% have right greater than left Coco expression, 0% have left greater than right, 68% are equal bilaterally and 0% are decreased bilaterally (n= 25). In TMEM195 knockdowns at stage 16, 22% have right greater than left Coco expression, 11% have left greater than right, 33% are equal bilaterally and 33% are decreased bilaterally (n = 18). In uninjected controls at stage 19, 96% have right greater than left Coco expression, 0% have left greater than right, 0% are equal bilaterally and 4% are decreased bilaterally. In TMEM195 knockdowns embryos at stage 19, 32% have right greater than left Coco expression, 6% have left greater than right, 10% are equal bilaterally and 51% are decreased bilaterally (n = 31). At stage 19, normal versus abnormal Coco expression is statistically significant

with $P < 0.0001$. Coco expression is therefore abnormal prior to nodal flow, suggesting abnormal formation of the GRP.

Xnr1 and Gdf6 are markers of the GRP (Figure 5d). I examined Xnr1 and Gdf6 expression starting at stages 14, and continuing through stages 16 and 19, like Coco. As shown in Figure 1d, Xnr1 showed decreased expression levels in comparison to the uninjected control, starting at stage 14 and continuing though stage 19. Gdf6 appear mildly decreased at stages 14 and 19, but became absent at stage 19. These preliminary results suggest abnormal formation of the GRP, suggesting the defect in left-right patterning is upstream of GRP formation.

Another important determinant of left-right development are cilia, which are immediately upstream of coco. Since the GRP appears to have formed abnormally, cilia on the GRP were examined to see if they were affected as well. Although the GRPs of morphants appeared ciliated, they appeared to have fewer cilia than the controls (Figure 5e). When counted, uninjected control embryos had 124 cilia per GRP ($n = 10$), while the TMEM195 knockdown embryos had 86 cilia per GRP ($n = 13$). This was a statistically significant difference between the two groups, with a p value < 0.001. This change in number of cilia could affect nodal flow and left-right patterning at the level of the GRP. However, given the abnormal formation of the GRP, signaling defects are likely also occurring earlier in development.

4.2 Gastrulation phenotype: high dose TMEM195 depletion causes gastrulation defects

Since a cardiac looping phenotype was seen with a 1ng dose of MO, I increased the dose in order to see if that would elicit a more penetrant LR phenotype. When 2ng of TMEM195 MO were injected, however, the embryos failed to gastrulate. I subsequently observed gastrulation of the 2ng injected embryos by time-lapse imaging and compared to the 1ng injected embryos and uninjected controls. As shown in figure 6a, the uninjected controls smoothly closed their blastopore and then folded their neural tubes. In contrast, time-lapse imaging showed that the 2ng injected embryos were unable to close their blastopores, despite multiple attempts. The 1ng injected embryos attempted several times to close their blastopore (typically 2 or more times). Their blastopores typically closed, or had a small opening, and then continued on to form their neural tubes.

In order to show that this gastrulation event was caused by TMEM195 depletion, I conducted a rescue experiment (Figure 6b). 99% of uninjected control embryos where able to gastrulate, with only 1% having open blastopore (n = 97). In contrast, only 21% of 2ng MO injected embryos were able to gastrulate, with 79% having open blastopores (n = 90). When 300pg of TMEM195 mRNA was injected after the 2ng MO, 60% were now able to gastrulate, with only 37% having open blastopores (n = 83). These results were statistically significant with $P < 0.001$.

As a control for this experiment, I injected TMEM195 mRNA into embryos on its own, to ensure that toxicity would not result (Figure 6c). When the rescue dose of

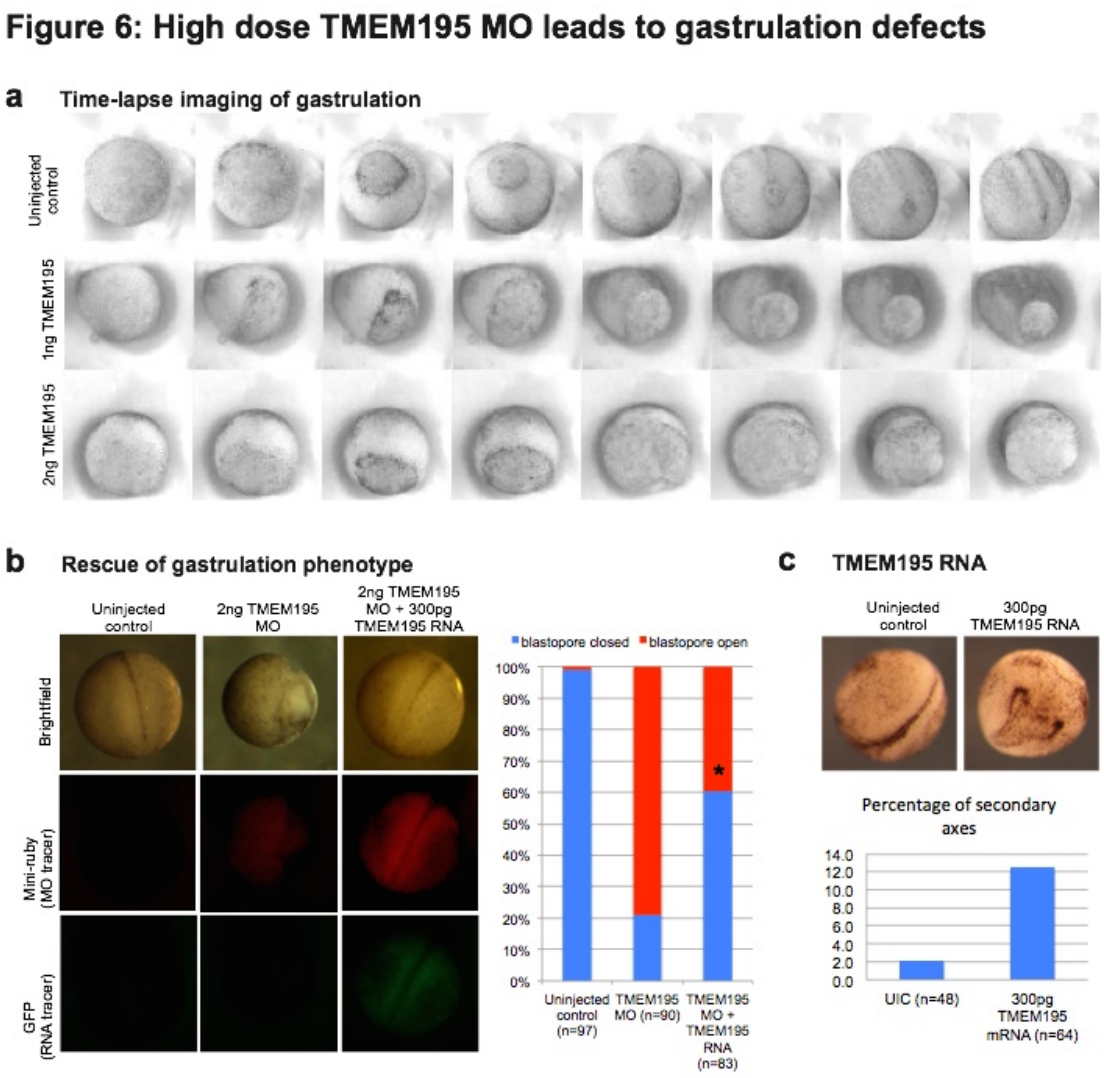

Figure 6: High dose TMEM195 depletion leads to heterotaxy

a) Time-lapse imaging of gastrulation. Uninjected control compared to 1ng and 2ng TMEM195 Mo injected embryos. b) Rescue of gastrulation phenotype. Uninjected control compared to 2ng TMEM195 MO injected embryos and 2ng TMEM195 Mo + 300pg TMEM195 mRNA. * Equal to $P < 0.001$. c) Overexpression of 300pg TMEM195 mRNA leads to secondary axis formation.

300pg was injected on its own into embryos, 13% of the mRNA embryos injected had secondary axes, in comparison to 2% of the uninjected control (UIC n = 48, TMEM195 mRNA n= 64, P = 0.09). Though these results were not statistically significant with a P = 0.09, the secondary axes were not anticipated, and this led to the hypothesis that either Wnt or BMP signaling may be affected by alterations in TMEM195 protein expression. Wnt and BMP pathways are two known ways that secondary axes can form. For example, overexpression of Wnt signaling leads to secondary axis formation (44). Given these overexpression results, I examined Wnt signaling first, in hopes of unraveling TMEM195's role in left-right development.

4.3 TMEM195 alteration affects the Wnt signaling pathway

In order to determine if TMEM195 expression alters Wnt signaling, I utilized TOPflash activity assays, western blots, and nuclear localization. A TOPflash assay shows the activity of TCF, the transcription factor that is bound by beta-catenin in the final steps of the Wnt signaling pathway. It is therefore a useful assay for showing changes in Wnt pathway activity (Figure 7a). When wild type beta-catenin is co-injected with the TOPflash reporter plasmid, a large peak forms with an activity ratio of 1.94 at stage 10 of development (3 biological replicates with 3 technical replicates per sample). In contrast, when both wild type beta-catenin and 2ng TMEM195 MO are co-injected with the reporter, the activity ratio is significantly lower at 0.73. In a separate experiment, TMEM195 mRNA was overexpressed in the TOPflash assay, and showed an activity ratio of 0.94, in comparison to beta-catenin

on its own, which had an activity ratio of 0.18 (3 biological replicates with 3 technical replicates per sample). The TOPflash assay confirmed the hypothesis that TMEM195 was altering Wnt signaling. In particular the results suggested that the alteration occurred at the level of beta-catenin rather than upstream (such as at the ligand or receptors). These experiments suggest that TMEM195 activates the Wnt signaling pathway at the level of beta-catenin, which could explain its role in gastrulation and secondary axis formation.

I next examined the effect of TMEM195 on endogenous levels of beta-catenin via western blotting (Figure 7b). At stage 10, at the initiation of gastrulation, the TMEM195 morphants had only 72% total beta-catenin, when compared to controls. At stage 12, beta-catenin decreased further in the morphants, to 35% of the controls ($p < 0.01$). These results show that endogenous levels of total beta-catenin are decreasing as the embryo gastrulates. Beta-catenin is necessary, as discussed in the introduction, for dorsal specification, which is where the initial involution of gastrulation occurs. Therefore, gastrulation initiates relatively normally and then fails, which is consistent with progressively decreasing levels of beta catenin during gastrulation.

The critical next question is, where in the Wnt pathway does TMEM195 exert its effects? In order to evaluate this, I performed a secondary axis assay (Figure 7c, 7d). The purpose of this assay is to overexpress different forms of beta-catenin, inducing secondary axes, and to see if I am able to reduce the number of embryos with secondary axes when I knock down TMEM195 in a subset. In this assay, I compared wild type beta-catenin to stabilized beta-catenin, and NLS tagged beta-

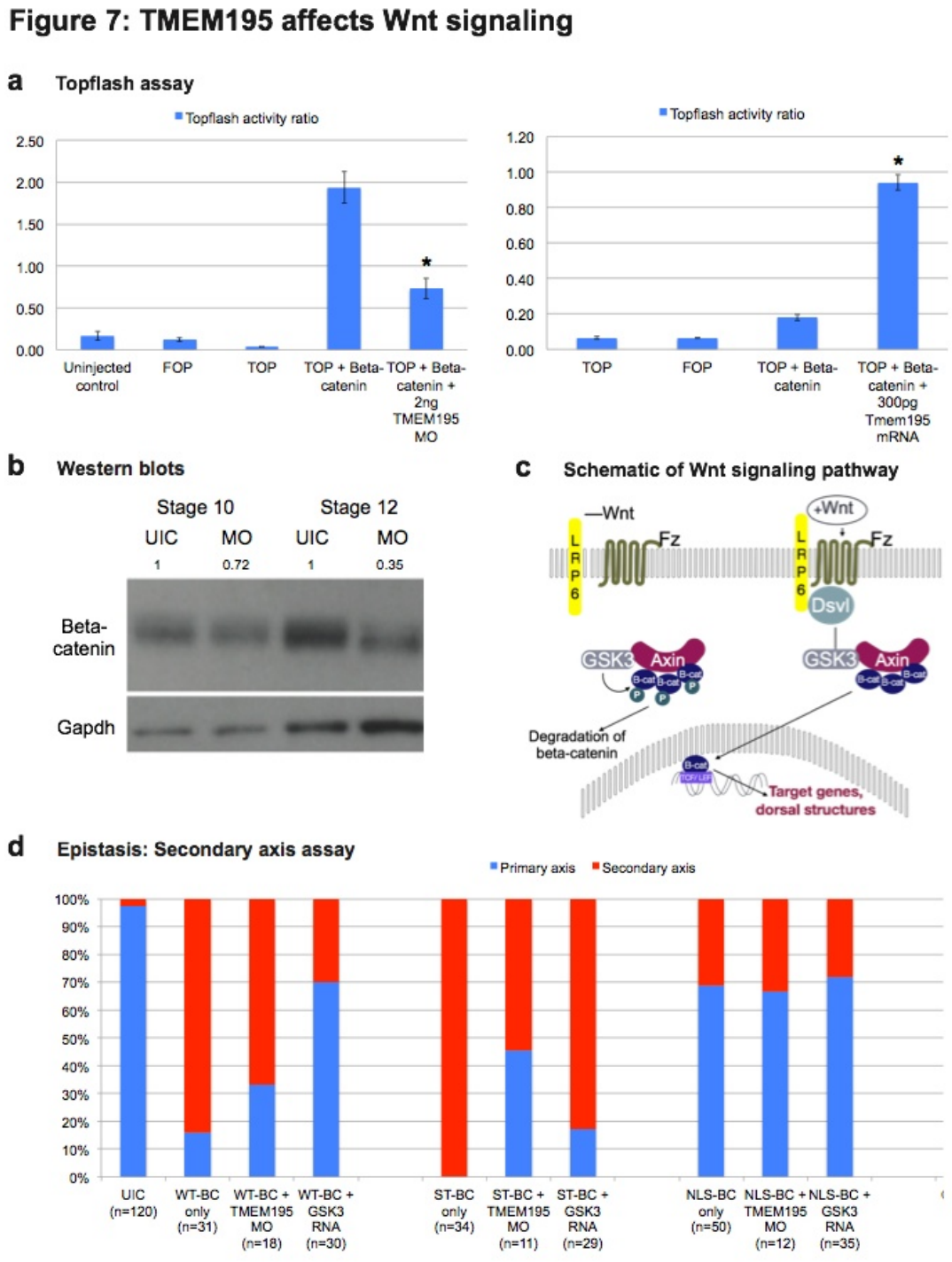

Figure 7: TMEM195 affects Wnt signaling

a) TOPflash assay of Wnt activity at stage 10 of development, comparing control embryos to depletion and overexpression of TMEM195. b) Western blot showing endogenous beta-catenin protein expression in control vs. knockdown embryos at stages 10 and 12 of development. c) Schematic of Wnt signaling pathway. d) Secondary axis assay comparing control vs. TMEM195 knockdown embryos. Each was co-injected wild type beta-catenin, stabilized-beta-catenin or NLS-beta-catenin.

catenin. Gsk3, which phosphorylates beta-catenin and targets it for degradation, was used throughout this experiment as a positive control. The results showed that WT-beta-catenin alone led to 84% secondary axes (n=18), while WT-beta-catenin + 1ng TMEM195 MO led to 67% secondary axes (n=18) and WT-beta-catenin + 200pg Gsk3 mRNA led to 30% secondary axes (n=30). In comparison, Stabilized beta-catenin alone led to 100% secondary axes (n=34), while ST-beta-catenin + 1ng TMEM195 MO led to 55% secondary axes (n=11) and ST-beta-catenin + 200pg Gsk3 mRNA led to 83% secondary axes (n=29) (overall $p<0.001$). The ability of GSK3 RNA overexpression to inhibit secondary axes caused by WT-beta-catenin but not those caused by ST-Beta-catenin acts as an important control in this experiment, and demonstrates that the stabilized construct is working as expected. These results demonstrate that depletion of TMEM195 can block Wnt signaling at the level of beta-catenin, even in the case of a stabilized form of beta-catenin. Therefore, it appears that TMEM195 does not exert its influence via the degradation of beta-catenin.

Since TMEM195 appears to block beta-catenin function despite stabilization, another hypothesis is that TMEM195 regulates beta-catenin nuclear transport. In order to test nuclear transport, I used an NLS-tagged beta-catenin in the secondary axis assay. The NLS tag provides a nuclear localization signal for beta-catenin, since no such known tag is present in the beta-catenin protein sequence. The purpose of this experiment is to see if beta-catenin is using an alternative route of entry into the nucleus, and if we can bypass that route by using an NLS signal. Embryos injected with only NLS-tagged beta-catenin were compared to those injected with NLS-beta-

catenin + 1ng TMEM195 MO and NLS-beta-catenin + 200pg GSK3 mRNA. All three had similar percentages of primary and secondary axes. In the NLS-beta-catenin embryos, only 69% had primary and 31% had secondary axes (n=50). In the NLS-beta-catenin + 1ng TMEM195 MO embryos 67% had primary and 33% had secondary axes (n=12). In the NLS-beta-catenin + 1ng TMEM195 MO embryos 72% had primary and 28% had secondary axes (n=35). Therefore, TMEM195 depletion appears ineffective in reducing the secondary axes induced by a beta-catenin with a canonical NLS signal. This demonstrates that beta-catenin nuclear localization can be rescued by employing the canonical nuclear import pathways and suggests that TMEM195 plays a critical role in the nuclear import of beta-catenin via an alternative, NLS independent, mechanism in the embryo.

4.4 TMEM195 is necessary for nuclear localization of beta-catenin

Given that NLS-beta-catenin appears to be unaffected in the secondary axis assay by TMEM195 depletion. We next sought to determine if TMEM195 affects the nuclear localization of beta-catenin by direct visualization.

First, I injected embryos with a GFP-tagged beta-catenin and NLS-mCherry and collected at stages 10 and 12 (Figure 8a). The GFP tag allows green visualization of the beta-catenin, and the mCherry tag allows red fluorescent visualization of the nucleus via the canonical nuclear transport pathway. At stage 10, the beginning of gastrulation, I saw both the GFP-beta-catenin and the NLS-mCherry in the nuclei. However, at stage 12, the end of gastrulation, only the NLS-mCherry was strongly

Figure 8: Nuclear localization of beta-catenin in TMEM195 morphants

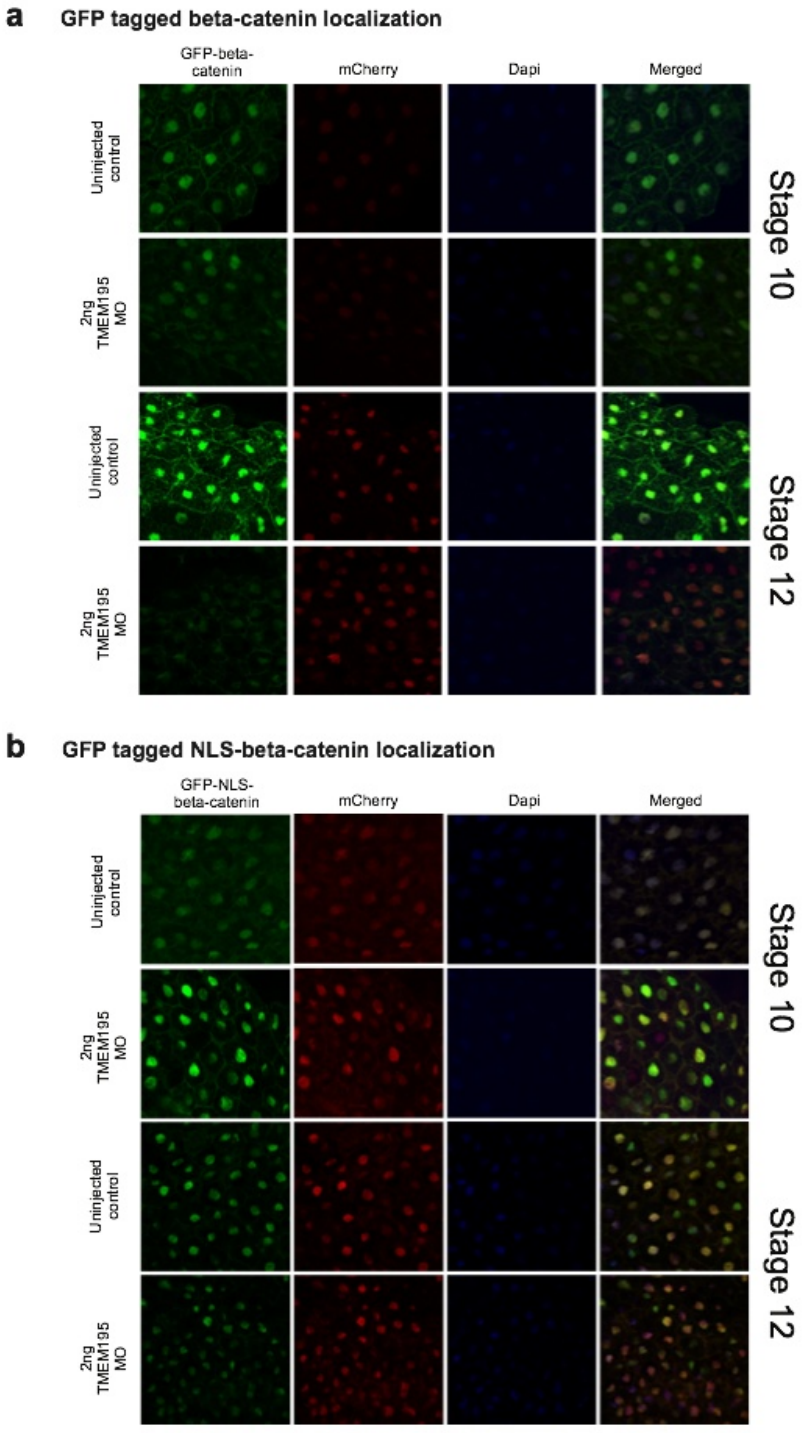

Figure 8: Nuclear localization of beta-catenin in TMEM195 morphants
a) Nuclear localization of GFP-beta-catenin with and without TMEM195 depletion at stage 10 and 12 of development. Embryos co-inject with NLS-mCherry. b) Nuclear localization of GFP-NLS-beta-catenin with and without TMEM195 depletion at stage 10 and 12 of development. Embryos co-inject with NLS-mCherry.

seen in the nuclei. In contrast, the GFP-tagged beta-catenin signal was significantly decreased. Consistent with our gastrulation phenotype and total levels of beta-catenin by western blot, the GFP-tagged beta-catenin is initially localized to the nucleus and then this is subsequently lost.

In the second nuclear localization experiment, I injected embryos with GFP tagged NLS-beta-catenin and NLS-mCherry, and once again collected at stages 10 and 12 (Figure 8b). At both stages 10 and 12, GFP and mCherry were both seen in the nuclei of the control embryos and in the nuclei of those co-injected with 2ng of TMEM195 MO. This shows that the NLS-tagged beta-catenin is able to enter the nucleus and that there is no additional inhibitory signal in beta-catenin which blocks nuclear localization in the knockdown of TMEM195.

Overall the nuclear localization results suggest that the NLS signal is necessary for beta-catenin entry into the nucleus when TMEM195 is depleted. This suggests that wild type beta-catenin may be using an alternative route of nuclear localization that is dependent on TMEM195 and that does not disrupt canonical nuclear import.

4.5 TMEM195 also regulates Smad2

My results suggest that while TMEM195 depletion affects the localization of beta-catenin, global nuclear import is not altered since both NLS-cherry and NLS-beta-catenin are readily detected in the nucleus. As described above, both Smad2 and Erk2 (in contrast to Smad1 and Erk1) lack canonical NLS signals but do have

armadillo repeats similar to beta-catenin. Like beta-catenin, the mechanism for their nuclear localization is unknown (5). Therefore, we hypothesized that nuclear localization of Smad2, but not Smad1, would also be affected by TMEM195 depletion (Figure 9). Embryos injected with 2ng of TMEM195 MO had 110% of the total value of total Smad1 at stage 10 and 100% at stage 11. These same embryos had 120% of phospho-Smad1 at stage 10 and 92% at stage 11. The results show slightly higher

Figure 9: Specificity of TMEM195

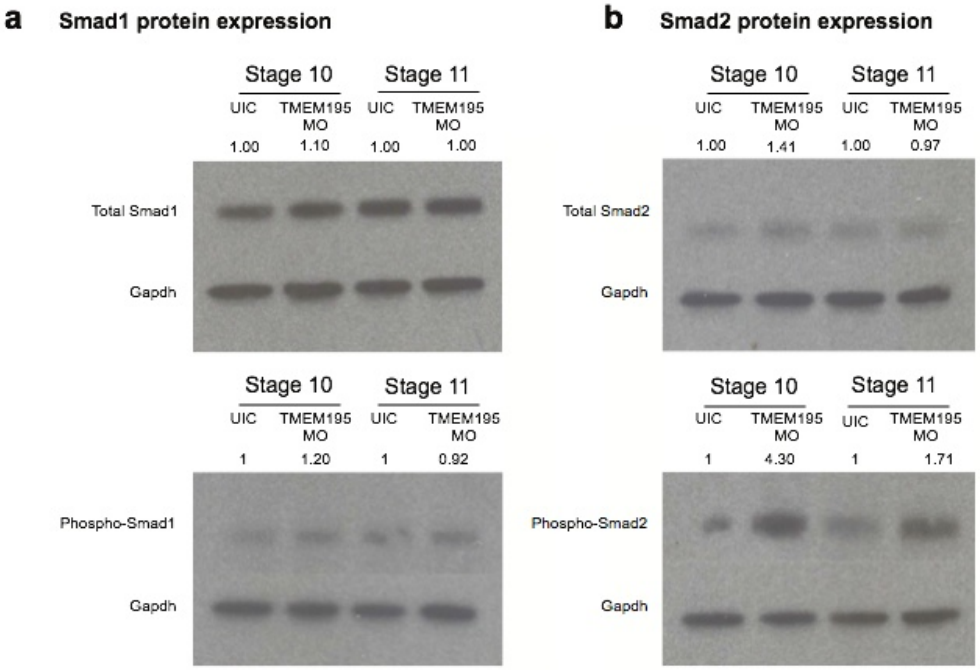

Figure 9: Specificity of TMEM195
a) Total and phospho-Smad1 protein expression at stages 10 and 11 of development. b) Total and phospho-Smad2 protein expression at stages 10 and 11 of development.

levels of both phospho- and total Smad1 at stage 10 in comparison to stage 11 in knockdown embryos, but the results were not significant with $p < 0.7$ and $p < 0.2$, respectively. Therefore, Smad1 appears unaffected by TMEM195 knockdown. In contrast, when I examined total Smad2, stage 10 knockdown embryos had 141% and stage 11 had 97% of the protein concentration of controls ($p < 0.07$). When phospho-Smad2 was examined, it showed a 430% increase in knockdown embryos at stage 10 and a 171% increase at stage 11 ($p < 0.001$). Overall, these results show a significant increase in phosphorylated Smad2 at stage 10 and at stage 11.

These results suggest that Smad2 but not Smad1 is affected by TMEM195 knockdown, resulting in an accumulation of phospho-Smad2 when TMEM195 is depleted. Whether this is due to an alteration in nuclear transport is not yet certain. I intend to pursue this further by tagging the Smads with GFP to examine nuclear localization. I am also starting to perform fractioning experiments; in which I isolate the cytoplasm from the nuclei in order to compare protein levels from each cellular compartment.

4.6 TMEM195's biochemical activity is important for mechanism

Previous experiments from the Werner lab discovered that TMEM195 has alkylglycerol monooxygenase (AGMO) activity. We wondered if this AGMO activity mediated the Wnt pathway. In order to test this, I injected wild type TMEM195 mRNA and the catalytically inactive mutants in which histidines were mutated to alanines at amino acid positions 136 and 149 (referred to as H136A and H149A).

The mRNAs were injected into embryos at the one cell stage, and then scored after neurulation for secondary axis formation (Figure 10c). Secondary axes were present in 15% of the standard TMEM195 mRNA injected embryos (n=53). In contrast, only 3% of uninjected control (n=157), 2% of H136A (n=44) and 3% of H149A (n=60) injected embryos had secondary axes ($p < 0.02$). This result suggests TMEM195's biochemical activity as an alkylglycerol monooxygenase may be the key to understanding its role in the Wnt signaling pathway.

4.7 TMEM195 is expressed predominately in dorsal structures

I performed TMEM195 *in-situ* hybridizations, which showed that TMEM195 RNA is strongly present in the animal poles in 4 and 8 cell embryos, and then becomes expressed circumferentially in stage 10 embryos (Figure 10a). In stage 19 embryos, TMEM195 is clearly present in the neural tube, and in stage 32 embryos it is prominent in the brachial arches, the brain and the spinal cord. In Stage 36 embryos, it is strongly present in the head and spinal cord. This expression pattern overall suggests that TMEM195 is important for dorsal structure formation, which is expected, given its demonstrated role in Wnt signaling.

4.8 TMEM195 localizes to the nuclear membrane

TMEM195 was previously localized to the endoplasmic reticulum in CHO cells by the Werner lab in Austria (4). However, my results suggest that TMEM195 has activity at the nuclear membrane. Since there is currently no known X*enopus*

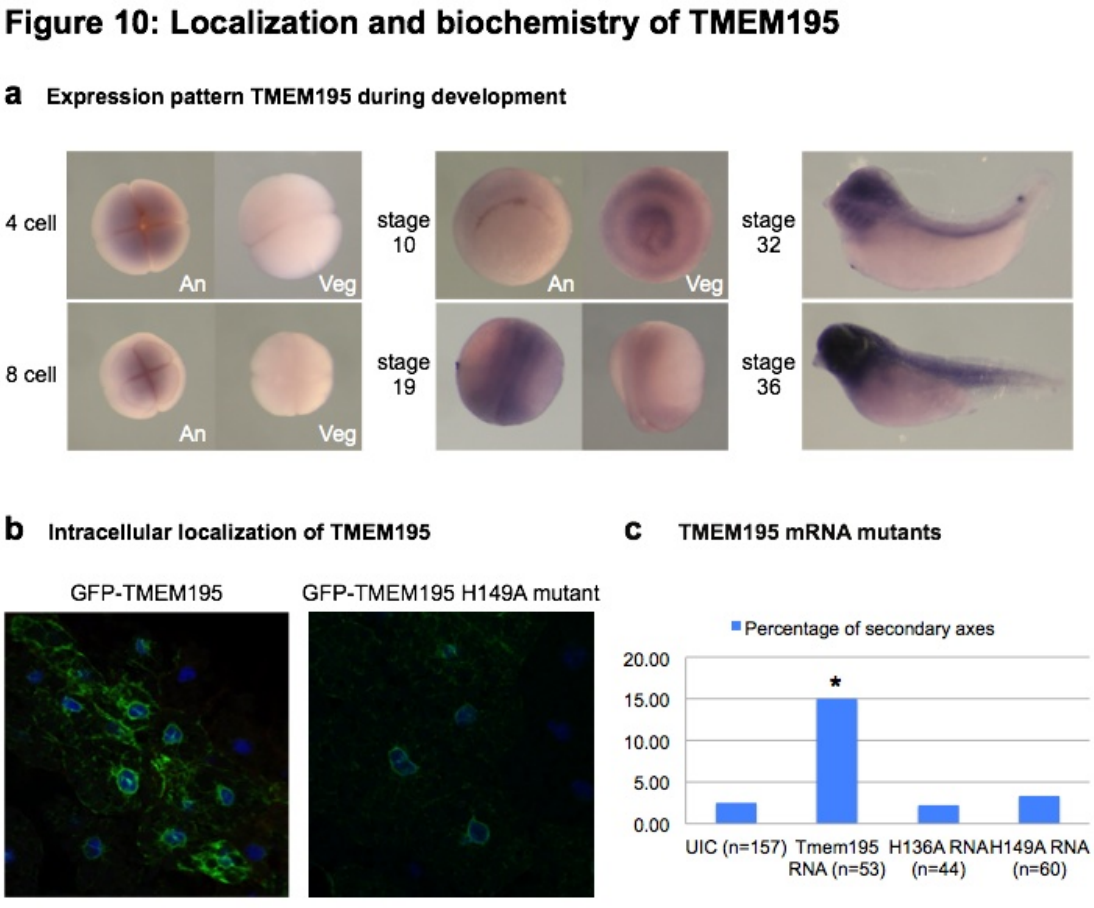

Figure 10: Localization and biochemistry of TMEM195
a) *In-situ* hybridization of wild type *Xenopus* embryos with TMEM195 probe shows strong dorsal expression. An, animal view; Veg, vegetal view. b) Intracellular localization of GFP-TMEM195 and GFP-TMEM195 H149A mutant in stage 10 embryos. Green is GFP and blue is DAPI. c) Secondary axis assay of overexpressed TMEM195 and TMEM195 mutants with $P < 0.02$.

antibody to TMEM195, in this experiment, I injected GFP-tagged TMEM195 mRNA into embryos and collected them at stage 10. The GFP-tagged mRNA was injected in doses ranging from 75-300pgs, and each dose showed clear nuclear localization (Figure 10b). The Werner lab also has several constructs with mutated histidines that are each essential for the biochemical activity of TMEM195. One of the mutant constructs, H149A, was injected into embryos. It was found to localize to the nuclear membrane as well.

Future experiments will try to co-localize TMEM195 and its mutant counterparts with a nuclear membrane marker, such as Laminin A, in order to verify that TMEM195 is at the nuclear envelope, and to identify where within the nuclear envelope it may be acting.

5.0 Discussion

TMEM195 is a newly described candidate gene for Htx in the developing human embryo. TMEM195 was originally identified by a copy number variant analysis in a patient with Htx. The index patient harbored a deletion of three exons overlapping the catalytic domain of TMEM195, potentially leading to an inactive form of the protein. Although no additional genetic information about the patient is available, it is hypothesized that this child was heterozygous for this mutation since our results suggest that TMEM195 deletions have a dose dependent response. If a small amount is deleted, cardiac looping defects can occur, but if slightly larger amounts are deleted, the embryo will not be able to gastrulate.

The patient's phenotype was recapitulated in *Xenopus tropicalis* embryos. With a low dose of the MO (1ng), depletion of TMEM195 results in Htx 22% of the time in this model system. TMEM195 knockdown also disrupted molecular markers of LR patterning including Pitx2 and Coco, as well as formation of the GRP, demonstrating that loss of TMEM195 affects the very earliest steps of LR development. Indeed a higher dose of MO leads to gastrulation defects, which suggests that an error during gastrulation may be the cause of the later developmental defects. Together, these findings demonstrate a role for TMEM195 in establishment of the embryonic LR axis and successfully complete specific aims 1A and 1B.

Initial experiments suggested that TMEM195 influenced Wnt signaling. A rescue experiment showed the specificity of the MO, proving that the gastrulation error was due to TMEM195 depletion. As a control for the rescue experiment, TMEM195 mRNA was injected on its own, resulting in secondary axis formation. Since excess Wnt signaling has been demonstrated to form secondary axes in *Xenopus* (44), the Wnt pathway was investigated by employing TOPflash assays. These data confirmed that Wnt signaling was significantly altered by TMEM195. If TMEM195 was knocked down, Wnt signaling activity was decreased in comparison to beta-catenin on its own. In contrast, if TMEM195 mRNA was added to the assay, TCF luciferase activity increased. This overexpression phenotype clearly increased Wnt signaling, which was consistent with secondary axis formation in the rescue experiment. Western blots showed similar results, confirming the effect of TMEM195 on endogenous levels of beta-catenin. Together these analyses

demonstrated that TMEM195 regulates Wnt signaling activity at the level of beta-catenin during gastrulation and also suggested that beta-catenin signaling was decreasing over time when TMEM195 was depleted. TMEM195's role may be developmental stage-dependent or may be due to decreasing maternal protein reserves.

To determine where in the Wnt signaling pathway TMEM195 is functioning, secondary axis assays and nuclear localization studies were performed. These data demonstrate that TMEM195 plays a role in nuclear transport. Experiments comparing wild type beta-catenin to NLS-tagged beta-catenin are the most striking. They show that NLS-tagged beta-catenin is able to enter the nuclei of TMEM195 depleted embryos, while wild type beta-catenin cannot. This result suggests that beta-catenin typically uses a non-NLS method of entry into the nucleus, which fits well with the existing literature (5, 49), and demonstrates that Tmem195 plays a key and somewhat specific role in this process as the NLS-tagged beta-catenin was able to bypass the defect in this non-canonical nuclear import route in Tmem195 morphants. Interestingly, embryos injected with NLS-beta-catenin were still unable to gastrulate. These data suggest that the defect caused by TMEM195 was not solely specific to Wnt signaling.

Phosphorylated-Smad2, a fellow transcription factor with no NLS tag and no known mechanism of nuclear entry, was increased by TMEM195 depletion. In contrast, TMEM195 depletion did not have any affect on Smad1, a transcription factor in the BMP signaling family that does contain an NLS signal. It is unknown if this increase in phosphorylated Smad2 reflects a defect in its nuclear import.

However, one possibility is that the nuclear import of Smad2 may be blocked, allowing more Smad2 to be phosphorylated in the cytoplasm in an effort to overcome a defect present in nuclear import.

Finally, the armadillo repeats on Smad2 and beta-catenin may allow them to bind to the FG repeats of nuclear pore proteins and then enter through the pore (5, 47). These armadillo repeats are structurally similar to heat repeats in importin-beta (5) and as such Smad2 and beta-catenin may be acting similarly to importin-beta in an alternative nuclear import pathway. TMEM195 affects nuclear import of beta-catenin and its depletion leads to increased levels of phospho-Smad2. Thus TMEM195 may be altering the nuclear import of both beta-catenin and Smad2 and possibly even other non-NLS transcription factors with similar armadillo structures, such as Erk2, a member of the MAP kinase family. The finding that TMEM195 localizes to the nuclear membrane supports this hypothesized role as well.

TMEM195's exact role in nuclear import is not well understood, however TMEM195's biochemical properties may be responsible. Overexpression of TMEM195 mRNA leads to secondary axis formation, suggesting increased Wnt activity. However, the catalytically dead mutant H136A and H149A forms of TMEM195 do not. These two alternative TMEM195's do not have the same biochemical properties, because each has one of the essential histidines replaced by an alanine. The enzymatic activities of TMEM195 are therefore key to its role in Wnt signaling.

TMEM195 can cleave ether lipids. Werner and colleagues have defined specific types of ether lipids that it might target. These include ether-containing GPI

anchors, the function of which is to tether proteins to the plasma membrane. TMEM195 may therefore cleave something that is tethered to the nuclear membrane. The specific target has yet to be discovered, but finding it may have a large impact, because it, like TMEM195, may play an essential role not only in Wnt signaling, but also in non-NLS transport. Non-classic NLS transport is very common and occurs in up to forty three percent of nuclear proteins (61). TGF-beta and MAP kinase are two examples of pathways with nuclear proteins lacking classical NLS transport. These are essential for normal embryonic development, cellular differentiation and proliferation. When genes in each of these pathways are mutated, cancer risks change, making it essential to understand each in order to fully understand normal and abnormal growth and development.

Prior to this study, no information was known about how TMEM195 affects development or nuclear signaling. In addition, despite the demonstrated role for beta-catenin and Smad2 signaling in cancer, stem cells, and embryonic development, the molecular regulators for the import of beta-catenin and Smad2 were largely unknown. One weakness of this study is a failure to confirm loss of nuclear localization of Smad2. I am currently trying to address this through nuclear and cytoplasmic protein fractions and through nuclear localization studies of GFP-tagged Smad2. A second weakness is that no antibody exists for TMEM195, making its localization dependent on a GFP-tagged construct. A third limitation is that the enzymatic target of TMEM195 has not yet been identified.

A newly described candidate Htx gene with both dose- and time-dependent features, TMEM195 variants result in LR patterning defects by decreasing beta-

catenin entry into the nucleus. This causes a decrease in the up-regulation of target dorsal genes necessary for formation of the left-right organizer. Smad2 signaling also appears dysregulated. This interaction and gradient of Smad2 and beta-catenin are necessary for organizer formation. As our results have shown, the left right organizer forms poorly in embryos with low dose depletion of TMEM195. In our patient, a reasonable hypothesis is that his or her LR organizer failed to form properly and was unable to properly determine asymmetry of the internal organs, leading to Htx.

Now that the putative role of TMEM195 in Htx has begun to be identified, the challenge is to identify TMEM195-associated health consequences. Wnt mutations greatly affect cancer risk. The patient may also be at risk for neurodevelopmental abnormalities, given that TMEM195 is strongly expressed in dorsal structures including the brain and spinal cord. Recent results from the Brueckner lab have shown that Htx genes expressed in the brain correlate with neurodevelopmental abnormalities when mutated in patients ((16) and unpublished data). Many questions remain, and highlight the importance of understanding the molecular pathways contributing to Htx and associated malformations. These genes may not only reveal how the LR axis of development forms, they may also provide important insight into new basic discoveries, such as non-NLS nuclear transport.

6.0 References

1. Watschinger K, and Werner ER. Alkylglycerol monooxygenase. *IUBMB life.* 2013;65(4):366-72.
2. van der Linde D, Konings EE, Slager MA, Witsenburg M, Helbing WA, Takkenberg JJ, and Roos-Hesselink JW. Birth prevalence of congenital heart disease worldwide: a systematic review and meta-analysis. *Journal of the American College of Cardiology.* 2011;58(21):2241-7.
3. Fakhro KA, Choi M, Ware SM, Belmont JW, Towbin JA, Lifton RP, Khokha MK, and Brueckner M. Rare copy number variations in congenital heart disease patients identify unique genes in left-right patterning. *Proceedings of the National Academy of Sciences of the United States of America.* 2011;108(7):2915-20.
4. Watschinger K, Keller MA, Golderer G, Hermann M, Maglione M, Sarg B, Lindner HH, Hermetter A, Werner-Felmayer G, Konrat R, et al. Identification of the gene encoding alkylglycerol monooxygenase defines a third class of tetrahydrobiopterin-dependent enzymes. *Proceedings of the National Academy of Sciences of the United States of America.* 2010;107(31):13672-7.
5. Xu L, and Massague J. Nucleocytoplasmic shuttling of signal transducers. *Nature reviews Molecular cell biology.* 2004;5(3):209-19.
6. Heron M, Hoyert DL, Murphy SL, Xu J, Kochanek KD, and Tejada-Vera B. Deaths: final data for 2006. *National vital statistics reports : from the Centers for Disease Control and Prevention, National Center for Health Statistics, National Vital Statistics System.* 2009;57(14):1-134.
7. Russo CA EA. In: Quality USAfHRa ed. *Statistical Brief*. Rockville, MD; 2007.
8. Warnes CA, Liberthson R, Danielson GK, Dore A, Harris L, Hoffman JI, Somerville J, Williams RG, and Webb GD. Task force 1: the changing profile of congenital heart disease in adult life. *Journal of the American College of Cardiology.* 2001;37(5):1170-5.
9. van der Bom T, Zomer AC, Zwinderman AH, Meijboom FJ, Bouma BJ, and Mulder BJ. The changing epidemiology of congenital heart disease. *Nature reviews Cardiology.* 2011;8(1):50-60.
10. Mussatto KA, Hoffmann RG, Hoffman GM, Tweddell JS, Bear L, Cao Y, and Brosig C. Risk and prevalence of developmental delay in young children with congenital heart disease. *Pediatrics.* 2014;133(3):e570-7.
11. Marino BS, Lipkin PH, Newburger JW, Peacock G, Gerdes M, Gaynor JW, Mussatto KA, Uzark K, Goldberg CS, Johnson WH, Jr., et al. Neurodevelopmental outcomes in children with congenital heart disease: evaluation and management: a scientific statement from the American Heart Association. *Circulation.* 2012;126(9):1143-72.
12. Brueckner M. Heterotaxia, congenital heart disease, and primary ciliary dyskinesia. *Circulation.* 2007;115(22):2793-5.
13. Swisher M, Jonas R, Tian X, Lee ES, Lo CW, and Leatherbury L. Increased postoperative and respiratory complications in patients with congenital

heart disease associated with heterotaxy. *The Journal of thoracic and cardiovascular surgery.* 2011;141(3):637-44, 44 e1-3.
14. Amula V, Ellsworth GL, Bratton SL, Arrington CB, and Witte MK. Heterotaxy syndrome: impact of ventricular morphology on resource utilization. *Pediatric cardiology.* 2014;35(1):38-46.
15. Zhu L, Belmont JW, and Ware SM. Genetics of human heterotaxias. *European journal of human genetics : EJHG.* 2006;14(1):17-25.
16. Zaidi S, Choi M, Wakimoto H, Ma L, Jiang J, Overton JD, Romano-Adesman A, Bjornson RD, Breitbart RE, Brown KK, et al. De novo mutations in histone-modifying genes in congenital heart disease. *Nature.* 2013;498(7453):220-3.
17. Yuan S, Zaidi S, and Brueckner M. Congenital heart disease: emerging themes linking genetics and development. *Current opinion in genetics & development.* 2013;23(3):352-9.
18. Amack JDaHJY. In: Harvey NRaRP ed. *Heart Development and Regeneration*. San Diego: Academic Press; 2010:p. 281-96.
19. Pierpont ME, Basson CT, Benson DW, Jr., Gelb BD, Giglia TM, Goldmuntz E, McGee G, Sable CA, Srivastava D, Webb CL, et al. Genetic basis for congenital heart defects: current knowledge: a scientific statement from the American Heart Association Congenital Cardiac Defects Committee, Council on Cardiovascular Disease in the Young: endorsed by the American Academy of Pediatrics. *Circulation.* 2007;115(23):3015-38.
20. Glessner JT, Bick AG, Ito K, Homsy JG, Rodriguez-Murillo L, Fromer M, Mazaika E, Vardarajan B, Italia M, Leipzig J, et al. Increased frequency of de novo copy number variants in congenital heart disease by integrative analysis of single nucleotide polymorphism array and exome sequence data. *Circulation research.* 2014;115(10):884-96.
21. Ransom J, and Srivastava D. The genetics of cardiac birth defects. *Seminars in cell & developmental biology.* 2007;18(1):132-9.
22. Boesgaard TW, Grarup N, Jorgensen T, Borch-Johnsen K, Meta-Analysis of G, Insulin-Related Trait C, Hansen T, and Pedersen O. Variants at DGKB/TMEM195, ADRA2A, GLIS3 and C2CD4B loci are associated with reduced glucose-stimulated beta cell function in middle-aged Danish people. *Diabetologia.* 2010;53(8):1647-55.
23. Renstrom F, Shungin D, Johansson I, Investigators M, Florez JC, Hallmans G, Hu FB, and Franks PW. Genetic predisposition to long-term nondiabetic deteriorations in glucose homeostasis: Ten-year follow-up of the GLACIER study. *Diabetes.* 2011;60(1):345-54.
24. Ramos E, Chen G, Shriner D, Doumatey A, Gerry NP, Herbert A, Huang H, Zhou J, Christman MF, Adeyemo A, et al. Replication of genome-wide association studies (GWAS) loci for fasting plasma glucose in African-Americans. *Diabetologia.* 2011;54(4):783-8.
25. Fujita H, Hara K, Shojima N, Horikoshi M, Iwata M, Hirota Y, Tobe K, Seino S, and Kadowaki T. Variations with modest effects have an important role in the genetic background of type 2 diabetes and diabetes-related traits. *Journal of human genetics.* 2012;57(12):776-9.

26. Goodarzi MO, Guo X, Cui J, Jones MR, Haritunians T, Xiang AH, Chen YD, Taylor KD, Buchanan TA, Hsueh WA, et al. Systematic evaluation of validated type 2 diabetes and glycaemic trait loci for association with insulin clearance. *Diabetologia.* 2013;56(6):1282-90.
27. Hong KW, Chung M, and Cho SB. Meta-analysis of genome-wide association study of homeostasis model assessment beta cell function and insulin resistance in an East Asian population and the European results. *Molecular genetics and genomics : MGG.* 2014;289(6):1247-55.
28. Akiyama K, Narita A, Nakaoka H, Cui T, Takahashi T, Yasuno K, Tajima A, Krischek B, Yamamoto K, Kasuya H, et al. Genome-wide association study to identify genetic variants present in Japanese patients harboring intracranial aneurysms. *Journal of human genetics.* 2010;55(10):656-61.
29. Dupuis J, Langenberg C, Prokopenko I, Saxena R, Soranzo N, Jackson AU, Wheeler E, Glazer NL, Bouatia-Naji N, Gloyn AL, et al. New genetic loci implicated in fasting glucose homeostasis and their impact on type 2 diabetes risk. *Nature genetics.* 2010;42(2):105-16.
30. Magnusson CD, and Haraldsson GG. Ether lipids. *Chemistry and physics of lipids.* 2011;164(5):315-40.
31. Blum M, Beyer T, Weber T, Vick P, Andre P, Bitzer E, and Schweickert A. Xenopus, an ideal model system to study vertebrate left-right asymmetry. *Developmental dynamics : an official publication of the American Association of Anatomists.* 2009;238(6):1215-25.
32. Wallingford JB, Liu KJ, and Zheng Y. Xenopus. *Current biology : CB.* 2010;20(6):R263-4.
33. Nonaka S, Shiratori H, Saijoh Y, and Hamada H. Determination of left-right patterning of the mouse embryo by artificial nodal flow. *Nature.* 2002;418(6893):96-9.
34. Okada Y, Takeda S, Tanaka Y, Izpisua Belmonte JC, and Hirokawa N. Mechanism of nodal flow: a conserved symmetry breaking event in left-right axis determination. *Cell.* 2005;121(4):633-44.
35. Lee JD, and Anderson KV. Morphogenesis of the node and notochord: the cellular basis for the establishment and maintenance of left-right asymmetry in the mouse. *Developmental dynamics : an official publication of the American Association of Anatomists.* 2008;237(12):3464-76.
36. Kawasumi A, Nakamura T, Iwai N, Yashiro K, Saijoh Y, Belo JA, Shiratori H, and Hamada H. Left-right asymmetry in the level of active Nodal protein produced in the node is translated into left-right asymmetry in the lateral plate of mouse embryos. *Developmental biology.* 2011;353(2):321-30.
37. Davis NM, Kurpios NA, Sun X, Gros J, Martin JF, and Tabin CJ. The chirality of gut rotation derives from left-right asymmetric changes in the architecture of the dorsal mesentery. *Developmental cell.* 2008;15(1):134-45.
38. Kurpios NA, Ibanes M, Davis NM, Lui W, Katz T, Martin JF, Izpisua Belmonte JC, and Tabin CJ. The direction of gut looping is established by changes in the extracellular matrix and in cell:cell adhesion. *Proceedings of the National Academy of Sciences of the United States of America.* 2008;105(25):8499-506.

39. Hamada H, and Tam PP. Mechanisms of left-right asymmetry and patterning: driver, mediator and responder. *F1000prime reports.* 2014;6(110.
40. Gilbert SF. *Developmental biology.* Sunderland, Mass.: Sinauer Associates; 2010.
41. Bilic J, Huang YL, Davidson G, Zimmermann T, Cruciat CM, Bienz M, and Niehrs C. Wnt induces LRP6 signalosomes and promotes dishevelled-dependent LRP6 phosphorylation. *Science.* 2007;316(5831):1619-22.
42. Kim SE, Huang H, Zhao M, Zhang X, Zhang A, Semonov MV, MacDonald BT, Zhang X, Garcia Abreu J, Peng L, et al. Wnt stabilization of beta-catenin reveals principles for morphogen receptor-scaffold assemblies. *Science.* 2013;340(6134):867-70.
43. Heasman J, Crawford A, Goldstone K, Garner-Hamrick P, Gumbiner B, McCrea P, Kintner C, Noro CY, and Wylie C. Overexpression of cadherins and underexpression of beta-catenin inhibit dorsal mesoderm induction in early Xenopus embryos. *Cell.* 1994;79(5):791-803.
44. McCrea PD, Brieher WM, and Gumbiner BM. Induction of a secondary body axis in Xenopus by antibodies to beta-catenin. *The Journal of cell biology.* 1993;123(2):477-84.
45. Kamato D, Burch ML, Piva TJ, Rezaei HB, Rostam MA, Xu S, Zheng W, Little PJ, and Osman N. Transforming growth factor-beta signalling: role and consequences of Smad linker region phosphorylation. *Cellular signalling.* 2013;25(10):2017-24.
46. Shen MM. Nodal signaling: developmental roles and regulation. *Development.* 2007;134(6):1023-34.
47. Xu L, Kang Y, Col S, and Massague J. Smad2 nucleocytoplasmic shuttling by nucleoporins CAN/Nup214 and Nup153 feeds TGFbeta signaling complexes in the cytoplasm and nucleus. *Molecular cell.* 2002;10(2):271-82.
48. Thrasivoulou C, Millar M, and Ahmed A. Activation of intracellular calcium by multiple Wnt ligands and translocation of beta-catenin into the nucleus: a convergent model of Wnt/Ca2+ and Wnt/beta-catenin pathways. *The Journal of biological chemistry.* 2013;288(50):35651-9.
49. Fagotto F, Gluck U, and Gumbiner BM. Nuclear localization signal-independent and importin/karyopherin-independent nuclear import of beta-catenin. *Current biology : CB.* 1998;8(4):181-90.
50. Sharma M, Jamieson C, Lui C, and Henderson BR. The hydrophobic rich N- and C-terminal tails of beta-catenin facilitate nuclear import of beta-catenin. *The Journal of biological chemistry.* 2014.
51. Heldin CH, and Moustakas A. Role of Smads in TGFbeta signaling. *Cell and tissue research.* 2012;347(1):21-36.
52. Shi Y, and Massague J. Mechanisms of TGF-beta signaling from cell membrane to the nucleus. *Cell.* 2003;113(6):685-700.
53. Tsukazaki T, Chiang TA, Davison AF, Attisano L, and Wrana JL. SARA, a FYVE domain protein that recruits Smad2 to the TGFbeta receptor. *Cell.* 1998;95(6):779-91.
54. Wu JW, Hu M, Chai J, Seoane J, Huse M, Li C, Rigotti DJ, Kyin S, Muir TW, Fairman R, et al. Crystal structure of a phosphorylated Smad2. Recognition of

phosphoserine by the MH2 domain and insights on Smad function in TGF-beta signaling. *Molecular cell.* 2001;8(6):1277-89.
55. Xu L, Chen YG, and Massague J. The nuclear import function of Smad2 is masked by SARA and unmasked by TGFbeta-dependent phosphorylation. *Nature cell biology.* 2000;2(8):559-62.
56. Varelas X, Sakuma R, Samavarchi-Tehrani P, Peerani R, Rao BM, Dembowy J, Yaffe MB, Zandstra PW, and Wrana JL. TAZ controls Smad nucleocytoplasmic shuttling and regulates human embryonic stem-cell self-renewal. *Nature cell biology.* 2008;10(7):837-48.
57. del Viso F, and Khokha M. Generating diploid embryos from Xenopus tropicalis. *Methods in molecular biology.* 2012;917(33-41.
58. Khokha MK, Chung C, Bustamante EL, Gaw LW, Trott KA, Yeh J, Lim N, Lin JC, Taverner N, Amaya E, et al. Techniques and probes for the study of Xenopus tropicalis development. *Developmental dynamics : an official publication of the American Association of Anatomists.* 2002;225(4):499-510.
59. Nieuwkoop PaFJ. Garland Pub.; 1994.
60. Sive HL GR, Harland RM. *Early Development of Xenopus Laevis: A laboratory Manual.* Cold Spring, NY: Cold Spring Harbor Laboratory Press; 2000.
61. Lange A, Mills RE, Lange CJ, Stewart M, Devine SE, and Corbett AH. Classical nuclear localization signals: definition, function, and interaction with importin alpha. *The Journal of biological chemistry.* 2007;282(8):5101-5.